MOMENT BASED OBJECT RECOGNITION AND RECONSTRUCTION

A THESIS SUBMITTED IN PARTIAL FULFILLMENT OF THE REQUIREMENTS FOR THE DEGREE OF

Master of Technology

In

Electronics System and Communication

By

SAIBAL DUTTA

Department of Electrical Engineering

National Institute of Technology

Rourkela

2007

MOMENT BASED OBJECT RECOGNITION AND RECONSTRUCTION

A THESIS SUBMITTED IN PARTIAL FULFILLMENT OF THE REQUIREMENTS FOR THE DEGREE OF

Master of Technology

In

Electronics System and Communication

By

Saibal Dutta

Under the Guidance of

Prof.P.K.Nanda

Department of Electrical Engineering

National Institute of Technology

Rourkela

2007

National Institute of Technology

Rourkela

CERTIFICATE

This is to certify that the thesis entitled, " **Moment Based Object Recognition and Reconstruction** " submitted by **Saibal Dutta** in partial fulfillment of the requirements for the award of Master of Technology Degree in **Electrical Engineering** with specialization in "**Electronics System and Communication**" at the National Institute of Technology, Rourkela (Deemed University) is an authentic work carried out by him under my supervision and guidance.

To the best of my knowledge, the matter embodied in the thesis has not been submitted to any other University/ Institute for the award of any degree or diploma.

Date:

Dr. Pradipta Kumar Nanda
(Professor & Head)
Dept. of Electrical Engg.
National Institute of Technology
Rourkela - 769008

ACKNOWLEGMENT

*I wish to express my deep and sincere gratitude towards my respectable guide and mentor **Prof. P.K Nanda** for his consistent and enthusiastic support throughout my thesis work, without his suggestions and ideas, this thesis would not be an asset for me. During my thesis work I feel the vibration of research only due the induction of vision and knowledge from my guide Prof P.K.Nanda.*

I would like to thanks all the faculties and staff of the Department of Electrical Engineering for their valuable suggestions and help during my M.Tech carrier.

I would like to thanks to my Maa, Baba, Didi and Jamaibabu for their support and understanding me during this thesis work.

I am indebted to the research scholars Mr. Priyadarshi Kanungo and Mrs. Sucheta Panda for their help towards the understanding of my thesis problem and work. I would like to thank M. Tech scholars Mr. Badri Narayan Subudhi and Mr.Rahul Dey for their appreciation and valuable questions which increases my understanding towards the problem. I am also grateful to all my batch mates and friends for their support and help.

I would like to thanks my IPCV lab which has provided me a great environment not only to build but to explore and grow.

Last but by no means least, as always I would like to thanks all those who are directly or indirectly supported and advised me during my thesis work.

Saibal Dutta
Roll No.20502003

Contents

List of Figures

List of Tables

Abstract

In this thesis,the problem of object recognition and reconstruction is addressed using image moments. Initially,scale,rotation and translation invariants properties of Geometric moments are studied.The central moments are translation invariants moments, are in used for object recognition. An object is recognised by its moments. The moments of an object and its differents occluded version are determined. An neural network is trained using above determined moments as the training set and target set corresponds to the moments of unoccluded object.The Artificial neural network(ANN) consider is feedforward network and back propagation algorithm is used to train the network.After training the moments of the differents of occluded object is used for prediction of the true moments.The predicted moments are matche with the orginal moments for object recognition.This is verified with different set of test images.The problem of object reconstruction using Zernike and Pseudozernike moments is also studied.The minimum order moments necessary for recostructing an object with minimum error is studied.

Chapter 1

INTRODUCTION

One of the basic problems in the design of an object recognition system relates to the selection of a set of appropriaet statistical features to be extracted from the object of interest for purpose of object classification.The recognition of object from image may be achieved with many methods by identifying an occluded object as a member of a set of known object.Efficient object recognition techniques taking characterization uniquely from objects representation. Research on use of moments purpose of object characterisation in both invariants and noninvariants tasks has received good topic in few decades. Mathematical concepts of moments has been utilized in many fields ranging from mechanics and statistics to pattern recognition and image understanding. Describing images with moments instead of other more commonly used image features, means the global properties of the image are used rather than local properties. Historically, the first significant work considering moments for pattern recognition was performed by Hu[1]. From method of algebric invariants, he derived a set of seven moment invariants, using non-linear combinations of geometric moments. These invariant remain the same under image translation, rotation and scaling. Since, then moments and functions of moments are widely used in pattern recognition, ship iden-

tification, aircraft identification, pattern matching and scene matching. In addition, the completeness of their description results in one of their cited attributes, the ability to reconstruction an object from its set of moments.

The fundamental theorem of moment invariants stated by Hu was infact incorrect. It was corrected by Reiss[2]. The error was only a slight one for it affects neither the scale invariance nor the rotation invariants but affect the features Hu proposed as being invariant to linear transformation. He has also introduced a new invariants which is invariant to change in illumination. Raveenderran, Jegannathan and Omatu[3] have proposed moment invariants that donot change in unequal scaling in X- and Y-directions. They have also tested it for mirror images. Suk and Flusser[4] have proposed radiometric invariants, which is invariant to change in intensity function and they have combined radio-metric geometric invariant. Tianxu and Jin[5] have used complex moment invariants to recognise blured images which are not affected by Gaussian bluring, rotation and scale of images.

Teh and Chin[6] have discussed different types of moments such as geometric or reguler moments, Legendre moments, Zernike moments, Pseudo-Zernike moments, Rotational moments and complex moments. They have also examined the properties of these moments and discussed the inter relationship among themselves. Besides these they have also discussed the image representation ability, noise sensitivity and information redundancy

It is easier to reconstruct the image from a set fo its orthogonal moments like Legendre, Zernike and Pseudo-Zernike moments than non orthogonal moments like Geometric,Rotational and Complex moments. A.Khotanzad and Y.H.Hong[7] have used Zernike moments for reconstruction of an image and also studied the invariance properties of Zernike moments. Like Zernike moments one can construct the image from the set of its Pseudo-Zernike mo-

ments. The reconstruction ability, noise sensitivity, information redundancy properties of Pseudo-Zernike moments[6] are better than that of Zernike moments, but the computation time of Pseudo-Zernike moments are more than that of Zernike moments.

One of the main difficulties concerning the use of Zernike moments as well as Pseudo-Zernike moments as features in image analysis applications is the high computation time to derive them. The long computation time to derive the Zernike as well as Pseudo-Zernike moments are due to the factorial terms present in the radial polynomials. The computation of factorial terms also leads to numerical instabilities for higher order moments. Hence it is required to compute the radial polynimials for both the Zernike and Pseudo-Zernike moments, which require less computation time.

Different authors[8][9][10] have been proposed different methods and algorithms to compute the radial polynomials. C. Wee, P.Raveendran and F. Takeda[9] have proposed hybrid algorithms to compute the Zernike radial polynomials. This algorithm takes less computation time to compute the Zernike radial polynomials than other methods. C. Chong, R. Mukundan and P.Raveendran[10] have proposed p-recursive method to compute the Pseudo-Zernike radial polynomials. Which is taking less computation time than other methods for computing the same. In recently,[13]proposed new type of moment,called Eigenmoments(EM)EM are obtained by performing eigen analysis in the moment space generated by geometric moments(GM).This is the transformation of the moment space in to the feature space where the signal to noise ratio(SNR) is maximized.Another different type of moments proposed by Ping [14]called Jacobi-Fourier Moments(JFM).It is one type of multi-distorted invariants orthogonal moments.

For accurate reconstruction, to get zero error, theoritically it requires infinity number of moments. Which is practically impossible for these above mentioned contineous orthogonal moments. They have also some difficulties like numerical approximation of continuous integrals, large variation in the dynamic range of values, coordinates space transformation, while implementing the moment functions. The above problem can be avoided by using discrete orthogonal polynomials as the basis set or kernel function, and to define the corresponding moments directly on the image coordinate space. Different discrete orthogonal polynomiala are Tchebuchef[11], Krawtchowk, Charlier, Meixner and Hann polynomials. Krawtchowk moments[12] can be employed to extract local features of an image, unlike other orthogonal moments which generally capture the global features.

The problem of object recognition using moments as investigated. Initially the invariance properties of such as translational scaling and rotation invariance of Geometric moments are translational invariant. This is studied in chapter2.

This invariance properties are exploited to study the object recognition. The first few low order moments together with the invariant moments are considered for recognition. The problem of recognition of a machine vision system for different degree of occlusion are computed. These moments together with the moments of the unoccluded objects are used as a training set for an Artificial Neural Network (ANN). The network is performed three layered network. The topology of the network is fixed by trial and error. The network is trained with the moments of a given object with a wide veriety of occlusions. The training of the network is achieved by Back Propagation(BP) algorithm. After training the moments of other occluded cases of the same object is used for prediction. The predicted value is compared with the orig-

inal moments of object and if the difference is withen a threshold, then the object recognition task is completed. This has been tested for indoor as well as outdoor images of gray as well as binary images. This is dealt in chapter3. The problem of image reconstruction using Zernike and Pseudo Zernike moments are studied in chapter4. It is observed that higher order moments are necessary (i.e even upto 50th order) for reconstruction of the image with less error. It is also observed that with the same order, the Pseudo Zernike moments yielded better results than that of using Zernike moments.

Chapter 2

INVARIANCE PROPERTIES OF MOMENTS

Moments and functions of moments have been utilized as pattern fetures in a number of applications to achieve invariant recognition of two-dimensional image pattern. The various applications of moments are for aircraft identification, scene matching, shape analysis, image normalization, character recognition,color texture recognition and image retrival as they are invariant to translation(shift), to change of scale and to rotation. Hence it is an important tool for image analysis. Hu[1] first introduced moment invariant in 1961, based on the method of algebric invariants. Using nonlinear combination of regular moments(geometric moments), he derived a set of invariant moments which has the desirable properties of being invariant under image translation, scaling and rotation. The fundamental theorem of moment invariants stated by Hu was in fact incorrect. It was corrected by Reiss[2]. The error was only a slight one, for it affects neither the scale invariants nor the rotation invariants but affect the features Hu presented as being invariant to linear transformation. He also introduced a new invariant which is invariant to change in illumination. Teh and Chin[6] have discussed different types of moments,their inter relationships and discussed in presence of noise.

Raveenderran, Jegannathan and Omatu[3] have proposed moment invariants that donot change in unequal scaling in X- and Y-directions. They have also tested it for mirror images. Suk and Flusser[4] have proposed radio-metric invariants, which is invariant to change in intensity function and they have combined radio-metric geometric invariants. Tianxu and Jin[5] have used complex moment invariants to recognise blured images, which are not affected by Gaussian bluring, rotation and scale of images.

Different types of moments, their invariants properties and their inter-relationships are discussed here. Invariant properties i.e. invariant to scale, translation and rotation of geometric moments and rotational invariant properties of Zernike moments are also examined here.

2.1 MOMENTS

2.1.1 General Definition of Moments

A general definition of moment functions ϕ_{pq} of order $(p+q)$ of an image intensity function $f(x,y)$ can be given as follows.

$$\phi_{pq} = \int_x \int_y \psi_{pq}(x,y) f(x,y) dx dy \tag{2.1}$$

Here we assume that the real image intensity function $f(x,y)$ is a piece wise contineous function and has bounded support. Where $\psi_{pq}(x,y)$ is the moment weighting kernel. The basis functions may have a range of useful properties that may be passed on to the moments, producing descriptions which can be invariant under rotation, scale and translation. To apply this to digital image, (2.1) need to be expressed in discrete form.

$$\phi_{pq} = \sum_x \sum_y \psi_{pq}(x,y) f(x,y) \tag{2.2}$$

Moreover, the orthogonality property of the basis function is passed on to the moments. Thus, non orthogonla basis functions result in non orthogonal moments and orthogonal basis functions result in orthogonal moments. Again orthogonal moments can be divided in to two parts i.e. contineous orthogonal moments and discrete orthogonal moments.

2.1.2 Geometric Moments

Geometric moments or regular moments[1] are the most popular types of moments and have been frequently used for a number of image processing tasks. Given the intensity function of an image $f(x, y)$, which is assumed to be piecewise contineous and with compact support, one can define the two dimentional geometric moments of order $(p + q)$ as.

$$m_{pq} = \int_{-\infty}^{+\infty} \int_{-\infty}^{+\infty} x^p y^q f(x, y) dx dy, \qquad p, q = 0, 1, 2, ... \tag{2.3}$$

The two-dimentional moment for a $(N \times N)$ discrete image is given by

$$m_{pq} = \sum_{-\infty}^{+\infty} \sum_{-\infty}^{+\infty} x^p y^q f(x, y) \tag{2.4}$$

The monomial product $x^p y^q$ is the basis function for this moment definition. However, the basis set $\{x^p y^q\}$ while complete(Weierstrass approximation theorem) is not orthogonal. Thus, geometric moments are not orthogonal since this basis function is not orthogonal.

Given the above assumption on $f(x, y)$ one can prove that moments of all order exists. This is known as ***existance theorem***. The infinite set of moments uniquely determines $f(x, y)$ and conversely are themselves uniquely determine by $f(x, y)$. This is known as ***uniqueness theorem***. These two theorems give rise to the reconstruction property of moments. It should be noted that the finiteness assumption is important, otherwise, the above uniqueness theorem meight not hold.

Moments of low orders can be used for normalizing the density distrubution function $f(x, y)$. The zero order moment m_{00} represents the total image power and can be used, in conjuction with the first order moments m_{10} and m_{01} to locate the centroid of the density distribution. Which is given by

$$\overline{x} = \frac{m_{10}}{m_{00}} \quad and \quad \overline{y} = \frac{m_{01}}{m_{00}} \tag{2.5}$$

The second order moments m_{20}, m_{02}, m_{11} characterise the size and orientation of image. So, the low order moments contain the most basic information regarding the shape size and orientation of the image.

Moment Generating Function

The moment generating function of $f(x, y)$ is defined as

$$M(u, v) = \int_{-\infty}^{+\infty} \int_{-\infty}^{+\infty} e^{(ux+vy)} f(x, y) dx dy \tag{2.6}$$

Where u and v are real. If moments of all order exists, then $M(u,v)$ can be expanded into a power series in terms of the moments m_{pq} as follows.

$$M(u, v) = \sum_{p=0}^{\infty} \sum_{q=0}^{\infty} m_{pq} \frac{u^p}{p!} \frac{v^q}{q!} \tag{2.7}$$

Central Moments

Central moments μ_{pq} are defined as

$$\mu_{pq} = \int_{-\infty}^{+\infty} \int_{-\infty}^{+\infty} (x - \overline{x})^p (y - \overline{y})^q f(x, y) dx dy, \quad p, q = 0, 1, 2, ... \tag{2.8}$$

Where $\overline{x}$ and $\overline{y}$ is given by(2.5).

The central moments are equivalent to the regular moments of an image that has been shifted such that the image centroid $(\overline{x}, \overline{y})$ coincide with the origin. As a result central moments are invariant to translation(shift) of the image.

For simplicity, it will be assumed that in the following that the origin has been choosen to coincide with the centroid of the image; therefore, μ_{pq} and $M(u,v)$ can be expressed as

$$\mu_{pq} = \int_{-\infty}^{+\infty} \int_{-\infty}^{+\infty} x^p y^q f(x,y) dxdy, \qquad p,q = 0,1,2,..... \tag{2.9}$$

$$M(u,v) = \sum_{p=0}^{\infty} \sum_{q=0}^{\infty} \mu_{pq} \frac{u^p}{p!} \frac{v^q}{q!} \tag{2.10}$$

2.1.3 Legendre Moments

The Legendre moments of order $(m+n)$ are defined as

$$\lambda_{mn} = \frac{(2m+1)(2n+1)}{4} \int_{-\infty}^{+\infty} \int_{-\infty}^{+\infty} P_m(x) P_n(y) f(x,y) dxdy \tag{2.11}$$

Where m,n=0,1,2,.....,∞ The Legendre polynomials $\{p_m(x)\}$ are a complete orthogonal basis set on the interval [-1,1].

$$\int_{-1}^{+1} p_m(x) p_n(x) dx = \frac{2}{2m+1} \delta_{mn} \tag{2.12}$$

The nth-order Lgendre polynomial is

$$p_n(x) = \sum_{j=0}^{n} a_{nj} x^j = \frac{1}{2^n n!} \frac{d^n}{dx^n} (x^2-1)^n \tag{2.13}$$

By the orthogonality principle, the image function $f(x,y)$ can be written as an infinite series expansion in terms of the Legendre polynomials over the square [-1$\leq x,y \leq$ 1]

$$f(x,y) = \sum_{m=0}^{\infty} \sum_{n=0}^{\infty} \lambda_{mn} p_m(x) p_n(y) \tag{2.14}$$

Where the Legendre moments $\{\lambda_{mn}\}$ are computed over the same square. If only Legendre moments of order $\leq$N are given; then the function $f(x,y)$ can be approximated by a continuous function which is a truncated series.

$$f(x,y) \approx \sum_{m=0}^{N} \sum_{n=0}^{m} \lambda_{m-n,n} p_{m-n}(x) p_n(y) \tag{2.15}$$

Using equations(2.3), (2.11) and (2.13) the Legendre moments and geometric moments are related by

$$\lambda_{mn} = \frac{(2m+1)(2n+1)}{4} \sum_{j=0}^{m} \sum_{k=0}^{n} a_{mj} a_{nk} M_{jk} \tag{2.16}$$

Thus, a given Legendre moment depends only on geometric moments of the same order and lower, and conversely.

2.1.4 Zernike Moments

The complex Zernike moments of order n with repetition l are defined as

$$A_{nl} = \frac{n+1}{\pi} \int_0^{2\pi} \int_0^1 [V_{nl}(r,\theta)]^*.f(r\ cos\theta,\ r\ sin\theta) r\ dr\ d\theta \tag{2.17}$$

Where $n = 0, 1, 2, ..., \infty$ and l takes on positive and negative integer values subject to the conditions $n - |l|$=even, and $|l| \leq n$. The symbol $*$ denotes the complex conjugate. The Zernike polynomials

$$v_{nl}(x,y) = V_{nl}(r\ cos\theta,\ r\ sin\theta) = R_{nl}(r) e^{il\theta} \tag{2.18}$$

are a complete set of complex-valued functions orthogonal on the unit disk $x^2 + y^2 \leq 1$

$$\int_0^{2\pi} \int_0^1 [V_{nl}(r,\theta)]^* V_{mk}(r,\theta) r\ dr\ d\theta = \frac{\pi}{n+1} \delta_{mn} \delta_{kl}. \tag{2.19}$$

The real valued radial polynomials $R_{nl}(r)$ satisfy the relations

$$\int_0^1 R_{nl}(r) R_{ml}(r) r dr = \frac{1}{2(n+1)} \delta_{mn} \tag{2.20}$$

and are defined as

$$R_{nl}(r) = \sum_{s=0}^{\frac{(n-|l|)}{2}} (-1)^s . \frac{(n-s)!}{s!(\frac{n+|l|}{2}-s)!(\frac{n-|l|}{2}-s)!} r^{n-2s} = \sum_{\substack{k=|l| \\ n-k=even}}^{n} B_{n|l|k} r^k. \tag{2.21}$$

The function $f(x,y)$ can be expanded in terms of the Zernike polynomials over the unit disk as

$$f(x,y) = \sum_{n=0}^{\infty} \sum_{\substack{l=-\infty \\ n-|l|=even \\ |l| \le n}}^{\infty} A_{nl} V_{nl}(x,y). \tag{2.22}$$

Where the zernike moments $\{A_{nl}\}$ are computed over the unit disk. If the series expansion is truncated at a finite order N, then the truncated expansion is the optimum approximation to $f(x,y)$.

$$f(x,y) \approx \sum_{n=0}^{N} \sum_{\substack{l \\ n-|l|=even \\ |l| \le n}}^{\infty} A_{nl} V_{nl}(x,y). \tag{2.23}$$

Because of the orthogonality of the Legendre and Zernike polynomials, both the Legendre moments $\{\lambda_{mn}\}$ and the Zernike moments $\{A_{nl}\}$ are in each case independent. It can be shown that Zernike moments and geometric moments are related by

$$A_{nl} = \frac{n+1}{\pi} \sum_{\substack{k=|l| \\ n-k=even}}^{n} \sum_{j=0}^{q} \sum_{m=0}^{|l|} w^m . \begin{pmatrix} q \\ j \end{pmatrix} . \begin{pmatrix} |l| \\ m \end{pmatrix} B_{n|l|k} M_{k-2j-m,2j+m} \tag{2.24}$$

where

$$w = \begin{cases} -i & if\ l > 0 \\ +i & if\ l \le 0 \end{cases} \tag{2.25}$$

$q = \frac{1}{2}(k-|l|)$, and $i = \sqrt{-1}$

2.1.5 Pseudo-Zernike Moments

Zernike polynomials, being invariant in form with respect to rotation of axis about the origin, are polynomials in x and y. A related orthogonal set of polynomials in x, y, and r which has the properties analogus to those of Zernike polynomials. These set of polynomials, which we shall call Pseudo-Zernike polynomials, differs from that of Zernike in that the real-valued radial polynomials are defined as

$$R_{nl}(r) = \sum_{s=0}^{n-|l|} (-1)^s . \frac{(2n+1-s)!}{s!(n-|l|-s)!(n+|l|+1-s)!} r^{n-s} = \sum_{k=|l|}^{n} S_{n|l|k} r^k . \tag{2.26}$$

Where now $n = 0, 1, 2, ..., \infty$ and l takes on positive and negative integer values subject to $|l| \leq n$ only. By simple enumeration, these set of Pseudo-Zernike polynomial contains $(n+1)^2$ linearly independent polynomials of degree $\leq n$, whereas the set of Zernike polynomials contains only $\frac{1}{2}(n+1)(n+2)$ linearly independent polynomials of degree $\leq n$ due to the additional condition $n-|l|$=even eliminated. Since the Pseudo-Zernike polynomials are also a complete set of functions orthogonal on the unit disk, both the series expansions of $f(x,y)$ in(2.22) and (2.23) hold with the conditions $n-|l|$=even eliminated, and $\{A_{nl}\}$ and $\{V_{nl}(x,y)\}$ are now the Pseudo-Zernike moments and the Pseudo-Zernike polynomial respectively. In addition, the Pseudo-Zernike moments are independent. Pseudo-Zernike moments are less sensitive to image noise than are the conventional Zernike moments.

2.1.6 Rotational Moments

The rotational moments of order n with repetition l are defined as

$$D_{nl} = \int_0^{2\pi} \int_0^{\infty} r^n e^{-il\theta} f(r\ cos\theta,\ r\ sin\theta) r\ dr\ d\theta \tag{2.27}$$

Where $i = \sqrt{-1}$, $n = 0, 1, 2, ..., \infty$ and l takes on positive and negative integer values. It can be shown that Zernike moments and rotational moments are related by

$$A_{nl} = \frac{n+1}{\pi} \sum_{\substack{k=|l| \\ n-k=even}}^{n} B_{n|l|k} D_{kl} \tag{2.28}$$

From which it follows that rotational moments can also be obtained from geometric moments by

$$D_{nl} = \sum_{j=0}^{q} \sum_{m=0}^{|l|} w^m . \begin{pmatrix} q \\ j \end{pmatrix} . \begin{pmatrix} |l| \\ m \end{pmatrix} M_{k-2j-m,2j+m} \tag{2.29}$$

where w is given by

$$w = \begin{cases} -i & if\ l > 0 \\ +i & if\ l \leq 0 \end{cases} \tag{2.30}$$

and $q = \frac{1}{2}(n - |l|)$. Unlike Legendre and Zernike moments, the rotational moments $\{D_{nl}\}$ are not independent.

2.1.7 Complex Moments

The complex moments of order $(p + q)$ are defined as

$$C_{pq} = \int_{-\infty}^{+\infty} \int_{-\infty}^{+\infty} (x + iy)^p (x - iy)^q f(x, y) dx dy \tag{2.31}$$

Where $p, q = 0, 1, 2, ..., \infty$, and $i = \sqrt{-1}$. The complex moment of order $(p + q)$ is a linear combination with complex coefficients of the geometric moments $\{M_{rs}\}$ satisfying $r + s = p + q$.

$$C_{pq} = \sum_{r=0}^{p} \sum_{s=0}^{q} \begin{pmatrix} p \\ r \end{pmatrix} . \begin{pmatrix} q \\ s \end{pmatrix} i^{p+q-(r+s)} . (-1)^{q-s} M_{r+s,p+q-(r+s)}. \tag{2.32}$$

In polar coordinates, the complex moment of order $(p+q)$ can be written as

$$C_{pq} = \int_0^{2\pi} \int_0^{\infty} r^{p+q} e^{i(p-q)\theta} f(r\ cos\theta,\ r\ sin\theta) r\ dr\ d\theta \tag{2.33}$$

Thus, it is related to the rotational moments as

$$D_{nl} = C_{\frac{1}{2}(n-l),\frac{1}{2}(n+l)} \tag{2.34}$$

from which it also follows that the Zernike moments and complex moments are related by

$$A_{nl} = \frac{n+1}{\pi} \sum_{\substack{k=|l| \\ n-k=even}}^{n} B_{n|l|k} C_{\frac{1}{2}(k-l),\frac{1}{2}(k+l)}. \tag{2.35}$$

The repetition of C_{pq} is defined as $p-q$. Like the rotational moments, the complex moments $\{C_{pq}\}$ are not independend.

2.2 MOMENT INVARIANTS

2.2.1 Algebric Forms and Invariants

The following homogeneous polynomial of two variables u and v[1],

$$f = a_{p0}u^p + \begin{pmatrix} p \\ 1 \end{pmatrix} a_{p-1,1}u^{p-1}v + \begin{pmatrix} p \\ 2 \end{pmatrix} a_{p-2,2}u^{p-2}v^2 + ... + \begin{pmatrix} p \\ p-1 \end{pmatrix} a_{1,p-1}uv^{p-1} + a_{0p}v^p \tag{2.36}$$

is called a binary algebric form, or simply a binary form, of order p. Using a notation, introduced by Cayley, the above form may be written as

$$f \equiv (a_{p0}; a_{p-1,1}; .....; a_{1,p-1}; a_{0p})(u,v)^p \tag{2.37}$$

A homogeneous polynomial $I(a)$ of the coefficients $a_{p0}, ..., a_{0p}$ is an algebric invariant of weight w, if

$$I(a'_{p0}, ..., a'_{0p}) = \Delta^w I(a_{p0}, ..., a_{0p}) \tag{2.38}$$

Where $a'_{p0}, ..., a'_{0p}$ are the new coefficients obtained from substituting the following general linear transformation into the original form(2.37).

$$\begin{pmatrix} u \\ v \end{pmatrix} = \begin{pmatrix} \alpha & \beta \\ \gamma & \delta \end{pmatrix} \begin{pmatrix} u' \\ v' \end{pmatrix}, \quad \Delta = \begin{vmatrix} \alpha & \beta \\ \gamma & \delta \end{vmatrix} \neq 0 \tag{2.39}$$

If $w = 0$, the invariant is called an absolute invariant; if $w \neq 0$ it is called a relative invariant. The invariant defined above may depend upon the coefficients of more than one form; Δ may not be limited to the determinant of the transformation. By eleminating Δ between two relative invariants, a non integral absolute invariant can always be obtained.

In the study of invariants, it is helpful to introduced another pair of variables x and y, whose transformation with respect to the above equation is as follows:

$$\begin{pmatrix} x' \\ y' \end{pmatrix} = \begin{pmatrix} \alpha & \beta \\ \gamma & \delta \end{pmatrix} \begin{pmatrix} x \\ y \end{pmatrix} \tag{2.40}$$

The transformation (2.40) is referred to as cogredient transformation, and (2.39) is referred to as contragredient transformation. The variable x and y are referred to as covariant variables, and u v as contravariant variables. They satisfies the following invariant relation

$$ux + vy = u'x' + v'y' \tag{2.41}$$

2.2.2 A Fundamental Theorem of Moment Invariants

The moment generating function with the exponential factor expanded into series form is

$$M(u, v) = \int_{-\infty}^{+\infty} \int_{-\infty}^{+\infty} \sum_{p=0}^{\infty} \frac{1}{p!}(ux + vy)^p f(x, y)dxdy \tag{2.42}$$

Interchanging the integration and summation process, we have

$$M(u, v) = \sum_{p=0}^{\infty} \frac{1}{p!}(\mu_{p0}, ..., \mu_{0p})(u, v)^p \tag{2.43}$$

By applying the transformation (40) to (42), and denoting the coefficient of $x^{'}$ and $y^{'}$ in transformed factor $(ux+vy)$ by $u^{'}$ and $v^{'}$, respectively we obtain

$$M_1(u^{'},v^{'}) = \int_{-\infty}^{+\infty}\int_{-\infty}^{+\infty}\sum_{p=0}^{\infty}\frac{1}{p!}(u^{'}x^{'}+v^{'}y^{'})^p f^{'}(x^{'},y^{'})\frac{1}{|J|}dx^{'}dy^{'} \tag{2.44}$$

Where $f^{'}(x^{'},y^{'}) \equiv f(x,y)$, $|J|$ is the absolute value of the Jacobian of the transformation(2.40), and $M_1(u^{'},v^{'})$ is the moment generating function after the transformation. If the transformed central moments $\mu^{'}_{pq}$ are defined as

$$\mu^{'}_{pq} = \int_{-\infty}^{+\infty}\int_{-\infty}^{+\infty}(x^{'})^p(y^{'})^q f^{'}(x^{'},y^{'})dx^{'}dy^{'}, \quad p,q = 0,1,2,..... \tag{2.45}$$

then we have

$$\begin{aligned} M_1(u^{'},v^{'}) &= \frac{1}{|J|}\sum_{p=0}^{\infty}\frac{1}{p!}(\mu^{'}_{p0},.....,\mu^{'}_{0p})(u^{'},v^{'})^p \\ &= \sum_{p=0}^{\infty}\frac{1}{p!}\left(\frac{\mu^{'}_{p0}}{|J|},.....,\frac{\mu^{'}_{0p}}{|J|}\right)(u^{'},v^{'})^p \end{aligned} \tag{2.46}$$

Equating coefficients we get

$$(\mu_{p0},.....,\mu_{0p})(u,v)^p = \left(\frac{\mu^{'}_{p0}}{|J|},.....,\frac{\mu^{'}_{0p}}{|J|}\right)(u^{'},v^{'})^p \tag{2.47}$$

Or

$$(|J|\mu_{p0},.....,|J|\mu_{0p})(u,v)^p = (\mu^{'}_{p0},.....,\mu^{'}_{0p})(u^{'},v^{'})^p \tag{2.48}$$

Fundamental Theorem: If the binary form of order p has an algebric invariant of weight w and order k

$$I(a^{'}_{p0},.....,a^{'}_{0p}) = \Delta^w I(a_{p0},.....,a_{0p}) \tag{2.49}$$

then the moments of order p have the invariant

$$I(\mu^{'}_{p0},.....,\mu^{'}_{0p}) = \Delta^w I(|J|\mu_{p0},.....,|J|\mu_{0p}) \tag{2.50}$$

$$I(\mu^{'}_{p0},.....,\mu^{'}_{0p}) = \Delta^w |J|^k(\mu_{p0},.....,\mu_{0p}) \tag{2.51}$$

This theorem holds also between algebric invariants containing coefficients from two or more forms of different orders and moment invariants containing moments of the corresponding orders.

2.2.3 Translation Invariants

Central moments are invariant to translation.The central moments are equivalent to the regular moments of an image that has been shifted such that the image centroid $(\overline{x}, \overline{y})$ coincide with the origin. As a result central moments are invariant to translation(shift) of the image. The central moments μ_{pq} is given by

$$\mu_{pq} = \int_{-\infty}^{+\infty} \int_{-\infty}^{+\infty} (x - \overline{x})_p (y - \overline{y})_q f(x, y) dx dy, \quad p, q = 0, 1, 2, ... \tag{2.52}$$

where $\overline{x} = \frac{m_{10}}{m_{00}}$ and $\overline{y} = \frac{m_{01}}{m_{00}}$

2.2.4 Scale Invariants

Under the similitude transformation, i,e, the change of size,

$$\begin{pmatrix} x^{'} \\ y^{'} \end{pmatrix} = \begin{pmatrix} \alpha & 0 \\ 0 & \alpha \end{pmatrix} \begin{pmatrix} x \\ y \end{pmatrix}, \quad \alpha = constant, \tag{2.53}$$

Each coefficient of any algebric form is an invariant

$$a_{pq}^{'} = \alpha^{p+q} a_{pq} \tag{2.54}$$

where α is not the determinant. For moment invariants we have

$$\mu_{pq}^{'} = \alpha^{p+q+2} \mu_{pq} \tag{2.55}$$

By eliminating α between the zeroth order relation,

$$\mu^{'} = \alpha^2 \mu \tag{2.56}$$

and the remaining ones, we have the following absolute similitude moment invariants:

$$\lambda_{pq} = \frac{\mu_{pq}^{'}}{(\mu^{'})^{(p+q+2)/2}} = \frac{\mu_{pq}}{\mu^{(p+q+2)/2}}, \quad p + q = 2, 3, ... \tag{2.57}$$

and

$$\mu_{10}^{'} = \mu_{01}^{'} \equiv 0 \tag{2.58}$$

2.2.5 Orthogonal Moment Invariants

Under the following proper following orthogonal transformation or rotation:

$$\begin{pmatrix} x' \\ y' \end{pmatrix} = \begin{pmatrix} cos\theta & sin\theta \\ -sin\theta & cos\theta \end{pmatrix} \begin{pmatrix} x \\ y \end{pmatrix} \tag{2.59}$$

We have

$$J = \begin{vmatrix} cos\theta & sin\theta \\ -sin\theta & cos\theta \end{vmatrix} = +1 \tag{2.60}$$

Therefore the moment invariant are exactly the same as the algebric invariants. If we treat the moments as the coefficients of an algebric form

$$(\mu_{p0}, ..., \mu_{0p})(u, v)^p \tag{2.61}$$

Under the following contragredient transformation:

$$\begin{pmatrix} u \\ v \end{pmatrix} = \begin{pmatrix} cos\theta & -sin\theta \\ sin\theta & cos\theta \end{pmatrix} \begin{pmatrix} u' \\ v' \end{pmatrix} \tag{2.62}$$

then we can derive the moment invariants by the following algebric method. If we subject both u, v and u' , v' to the following transformation:

$$\begin{pmatrix} U \\ V \end{pmatrix} = \frac{1}{2} \begin{pmatrix} 1 & i \\ 1 & -i \end{pmatrix} \begin{pmatrix} u \\ v \end{pmatrix}, \tag{2.63}$$

$$\begin{pmatrix} U' \\ V' \end{pmatrix} = \frac{1}{2} \begin{pmatrix} 1 & i \\ 1 & -i \end{pmatrix} \begin{pmatrix} u' \\ v' \end{pmatrix} \tag{2.64}$$

then the orthogonal transformation is converted into the following simple relations,

$$U' = Ue^{-i\theta}, \quad V' = Ve^{i\theta} \tag{2.65}$$

We have the following identities:

$$(I_{p0}, ..., I_{0p})(U, V)^p \equiv (\mu_{p0}, ..., \mu_{0p})(u, v)^p$$

$$\equiv (\mu'_{p0}, ..., \mu'_{0p})(u', v')^p$$

$$\equiv (I'_{p0}, ..., I'_{0p})(Ue^{-i\theta}, Ve^{-i\theta})^p, \tag{2.66}$$

Where $I_{p0}, ..., I_{0p}$ and $I'_{p0}, ..., I'_{0p}$ are the corresponding coefficients after the substitutions. From the identity in U and V, the coefficients of various monomials $U^{p-r}V^r$ on the sides must be the same. Therefore,

$$I'_{p0} = e^{ip\theta}I_{p0}; \quad I'_{p-1,1} = e^{i(p-2)\theta}I_{p-1,1}; .....;$$

$$I'_{1,p-1} = e^{-i(p-2)\theta}I_{1,p-1}; I'_{0p} = e^{-ip\theta}I_{0p}. \tag{2.67}$$

These are $(p+1)$ linearly independent moment invariants under proper orthogonal transformations, and $\Delta = e^{i\theta}$ which is not the determinant of the transformation. From the identity of first two expressions, it can be seen that $I_{r,p-r}$ is the complex conjugate of $I_{p-r,r}$.

$$I_{p0} = \mu_{p0} - i\begin{pmatrix} p \\ 1 \end{pmatrix}\mu_{p-1,1} - \begin{pmatrix} p \\ 2 \end{pmatrix}\mu_{p-2,2} + i\begin{pmatrix} p \\ 3 \end{pmatrix}\mu_{p-3,3} + ... + (-i)^p\mu_{0p},$$

$$I_{p-1,1} = (\mu_{p0} + \mu_{p-2,2}) - i(p-2)(\mu_{p-1,1} + \mu_{p-3,3}) + ... + (-i)^{p-2}(\mu_{2,p-2} + \mu_{0p}),$$

$$I_{p-2,2} = (\mu_{p0} + 2\mu_{p-2,2} + \mu_{p-4,4}) - i(p-4)(\mu_{p-1,1} + 2\mu_{p-3,3} + \mu_{p-5,5}) + ...$$

$$.. + (-i)^{p-4}(\mu_{4,p-4} + 2\mu_{2,p-2} + \mu_{0p}),$$

$$I_{p-r,r} = [(\mu_{p0}; \mu_{p-2,2}; .....; \mu_{p-2r,2r})(1,1)^r;$$

$$(\mu_{p-1,1}; \mu_{p-3,3}; .....; \mu_{p-2r-1,2r+1})(1,1)^r; ....;$$

$$(\mu_{2r,p-2r}; \mu_{2r+2,p-2r-2}; .....; \mu_{0p})(1,1)^r](1,-i)^{p-2r}, \quad p-2r > 0 \tag{2.68}$$

and

$$I_{p/2,p/2} = \mu_{p0} + \begin{pmatrix} p/2 \\ 1 \end{pmatrix}\mu_{p-2,2} + \begin{pmatrix} p/2 \\ 2 \end{pmatrix}\mu_{p-4,4} + ... + \mu_{0p}, \quad p = even \tag{2.69}$$

It may be noted that these $(p+1)$ I's are linearly independent linear functions of the μ's, and vice versa.

For the following improper orthogonal transformation, *i.e.*, rotation and reflection:

$$\begin{pmatrix} x' \\ y' \end{pmatrix} = \begin{pmatrix} cos\theta & sin\theta \\ sin\theta & -cos\theta \end{pmatrix} \begin{pmatrix} x \\ y \end{pmatrix}, \quad \begin{vmatrix} cos\theta & sin\theta \\ sin\theta & -cos\theta \end{vmatrix} = -1 \tag{2.70}$$

Similarly, we have

$$U' = Ve^{i\theta}, \quad V' = Ue^{-i\theta} \tag{2.71}$$

and

$$I'_{p0} = e^{-ip\theta} I_{0p}; \quad I'_{p-1,1} = e^{-i(p-2)\theta} I_{1,p-1}; \ldots\ldots\ldots;$$
$$I'_{1,p-1} = e^{i(p-2)\theta} I_{p-1,1}; I'_{0p} = e^{ip\theta} I_{p0}. \tag{2.72}$$

Where $I_{p0}, \ldots\ldots, I_{0p}$ and $I'_{p0}, \ldots\ldots, I'_{0p}$ are the same as those given by (2.68)

2.2.6 A Complete System of Absolute Orthogonal Moment Invariants

From (2.67) and (2.72), we may derive the following system of moment invariants by eliminating the factor $e^{i\theta}$

For the second-order moments, the two independent invariants are

$$I_{11}, \qquad I_{20}I_{02}. \tag{2.73}$$

For the third-order moments, the three independent invariants are

$$I_{30}I_{03}, \qquad I_{21}I_{12},$$
$$(I_{30}I_{12}^3 + I_{03}I_{21}^3). \tag{2.74}$$

A fourth one dependending also on the third order moments only is

$$\frac{1}{i}(I_{30}I_{12}^3 - I_{03}I_{21}^3) \tag{2.75}$$

There exists an algebric relation between the above four invariants given in (2.74) and(2.75) . The first three given by (2.74) are absolute invariants for both proper and improper rotations but the last one goven by(2.75) is invariant under proper rotation, and changes sign under improper rotation. This will be called a skew invariant. Therefore it is useful for distinguishing morror images One more independent absolute invariant may be formed from second and third order moments as follows:

$$(I_{20}I_{12}^2 + I_{02}I_{21}^2) \tag{2.76}$$

For pth order moments,$p > 4$ we have $[p/2]$, the integral part of $p/2$, invariants

$$I_{p0}I_{0p}; \quad ; I_{p-1,1}I_{1,p-1}; \quad ; I_{p-r,r}I_{r,p-r}; ..... \tag{2.77}$$

If p is even, we also have

$$I_{p/2,p/2} \tag{2.78}$$

And also combined with $(p-2)$th order moments, we have $[p/2-1]$ invariants

$$\begin{gathered}(I_{p-1,1}I_{0,p-2} + I_{1,p-1}I_{p-2,0}),\\ (I_{p-2,2}I_{1,p-3} + I_{1,p-1}I_{p-2,0}), ...\\ (I_{p-r,r}I_{r-1,p-r+1} + I_{r,p-r}I_{p-r+1,r-1}), ...p-2r > 0\end{gathered} \tag{2.79}$$

Wheather p is odd or even we always have $(p+1)$ independent absolute invariants. By changing the above sum into differences we get skew invariants. All the independent moment invariants together form a complete system, for any given invariant, it is always possible to express it in terms of the above invariants.

For the second and third order moments, we have the following six absolute orthogonal invariants:

$$\phi_1 = \mu_{20} + \mu_{02} \tag{2.80}$$

$$\phi_2 = (\mu_{20} - \mu_{02})^2 + 4\mu_{11}^2 \tag{2.81}$$

$$\phi_3 = (\mu_{30} - 3\mu_{12})^2 + (3\mu_{21} - \mu_{03})^2 \tag{2.82}$$

$$\phi_4 = (\mu_{30} + \mu_{12})^2 + (\mu_{21} + \mu_{03})^2 \tag{2.83}$$

$$\phi_5 = (\mu_{30} - 3\mu_{12})(\mu_{30} + \mu_{12})[(\mu_{30} + \mu_{12})^2 - 3(\mu_{21} + \mu_{03})^2]$$

$$+(3\mu_{21} - \mu_{03})(\mu_{21} + \mu_{03}).[3(\mu_{30} + \mu_{12})^2 - (\mu_{21} + \mu_{03})^2] \tag{2.84}$$

$$\phi_6 = (\mu_{20}-\mu_{02})[(\mu_{30}+\mu_{12})^2-(\mu_{21}+\mu_{03})^2]+4\mu_{11}(\mu_{30}+\mu_{12})(\mu_{21}+\mu_{03}) \tag{2.85}$$

and one skew orthogonal invariants,

$$\phi_7 = (3\mu_{21} - \mu_{03})(\mu_{30} + \mu_{12})[(\mu_{30} + \mu_{12})^2 - 3(\mu_{21} + \mu_{03})^2]$$

$$-(\mu_{30} - 3\mu_{12})(\mu_{21} + \mu_{03}).[3(\mu_{30} + \mu_{12})^2 - (\mu_{21} + \mu_{03})^2] \tag{2.86}$$

This skew invariant is useful in distinguishing mirror images. The above mentioned invariants are commonly known as Hu's invariants.

2.2.7 Moment Invavariants Under Unequal Scaling

The conventional regular moments can be defined as[3]:

$$m_{pq} = \int_{-\infty}^{+\infty} \int_{-\infty}^{+\infty} x^p y^q f(x,y) dx dy, \quad p,q = 0,1,2,..... \tag{2.87}$$

Usually these moments are made invariant to translation and scaling by forming the following invariants:

$$\lambda_{pq} = \frac{\mu_{pq}}{m_{00}^{(p+q+2)/2}} \quad p,q = 0,1,2,..... \tag{2.88}$$

Where

$$\mu_{pq} = \int_{-\infty}^{+\infty} \int_{-\infty}^{+\infty} (x-\overline{x})^p (y-\overline{y})^q f(x,y) dx dy, \quad p,q = 0,1,2,.... \tag{2.89}$$

and

$\overline{x} = \frac{m_{10}}{m_{00}}$ and $\overline{y} = \frac{m_{01}}{m_{00}}$.

Consider the unequal scaled image. It is related to original image as

$$g(x, y) = f(ax, by) \tag{2.90}$$

If now λ_{pq} is evaluated for $g(x, y)$, we obtain

$$\overline{\lambda}_{pq} = r^{(p-q)/2}\lambda_{pq} \qquad for \;\; p,\; q = 0, 1, 2, ... \tag{2.91}$$

In the above equation, the sign '-' denites the moment formed using $g(x, y)$ and $r = a/b$; a and b are the scaling constant in the x and y direction respectively. If $r = 1$ then $\overline{\lambda}_{pq}$ is same as λ_{pq}. For $r \neq 0$

$$\overline{\mu}_{pq} = \frac{1}{a^{p+1}b^{q+1}}\mu_{pq} \qquad p,\; q = 0, 1, 2, ... \tag{2.92}$$

2.2.8 Blur Invariants

An important class of radiometric degradations we are faced with often in practice is image bluring[4][5]. Bluring can be caused by camera defocus, atmospheric turbulance etc. If the scene is flat, bluring can be ususlly described by a convolution

$$g(x, y) = f(x, y) \otimes h(x, y) \tag{2.93}$$

where $f(x, y)$ is an original(ideal) image, $g(x, y)$ is an accuired image and $h(x, y)$ is a point spread function(PSF) of the image system. Since in most practical tasks the PSF is unknown, having invariant to convolution is of prime importance when recognizing objects in a blured scene.

theorem: Let $f(x, y)$ be an image function. Let us define the following function $C^{(f)} : N_0 \times N_0 \to R$. If $(p + q)$ is even then

$$C(P, Q)^{(f)} = 0 \tag{2.94}$$

If $(p+q)$ is odd then $C(P,Q)^{(f)} = \mu_{pq}^{f} -$

$$\frac{1}{\mu_{00}} \sum_{n=0}^{p} \sum_{\substack{m=0 \\ 0<m+n<p+q}}^{q} \binom{p}{n} \binom{p}{n} C(p-n, q-m)^{(f)} . \mu_{nm}^{(f)} \quad (2.95)$$

Then $C(p,q)^{(f)}$ is invariant to convolution with any centrosymmetric function $n(x,y)$, i.e.

$$C(p,q)^{(f)} = C(p,q)^{(f \star h)} \quad (2.96)$$

for any p and q.

As an example, for a Gaussian point spread function can be defined as

$$h(x,y) = \frac{1}{2\pi\sigma^2} e^{\frac{x^2+y^2}{2\sigma^2}} \quad (2.97)$$

theorem: In a complex moment C_{pq}, as long as at least one of the subscripts (p or q) is zero it will not be affected by Gaussian bluring.

In special case it can be proved that C_{12} and C_{21} are also invariant to Gaussian bluring, though there is neither p nor q is zero.

2.2.9 Rotational Invariant Features of Zernike Moments

Consider a rotation of the image through an angle α. If the rotated image is denoted by f^r, the relationship between the original and rotated image in the same polar coordinate is

$$f^r(\rho, \theta) = f(\rho, \theta - \alpha) \quad (2.98)$$

From the definition, the zernike moments of the original image is given by

$$\begin{aligned} A_{nl} &= \frac{n+1}{\pi} \int_0^{2\pi} \int_0^1 f(\rho,\ \theta) . [V_{nl}(\rho,\theta)]^* \rho \, d\rho \, d\theta \\ &= \frac{n+1}{\pi} \int_0^{2\pi} \int_0^1 f(\rho,\ \theta) . R_{nl}(\rho) e^{-jl\theta} \rho \, d\rho \, d\theta \end{aligned} \quad (2.99)$$

The Zernike moment of the rotated image in the same coordinate is

$$A_{nl}^{r} = \frac{n+1}{\pi} \int_0^{2\pi} \int_0^1 f(\rho,\ \theta - \alpha).R_{nl}(\rho) e^{-jl\theta} \rho\ d\rho\ d\theta \tag{2.100}$$

By achange of variable $\theta_1 = \theta - \alpha$

$$\begin{aligned} A_{nl}^{r} &= \frac{n+1}{\pi} \int_0^{2\pi} \int_0^1 f(\rho,\ \theta_1).R_{nl}(\rho) e^{-jl(\theta_1+\alpha)} \rho\ d\rho\ d\theta_1 \\ &= \left[\frac{n+1}{\pi} \int_0^{2\pi} \int_0^1 f(\rho,\ \theta_1).R_{nl}(\rho) e^{(-jl\theta_1)} \rho\ d\rho\ d\theta_1\right] e^{(-jl\alpha)} \\ &= A_{nl}.e^{(-jl\theta)} \end{aligned} \tag{2.101}$$

The above equation shows that Zernike moments have simple rotational transformation properties; each Zernike moments merely acquires a phase shift on rotation. This simple property leads to the conclusion that the magnitude of the Zernike moments of the rotated image function remain identical to those before rotation. Thus $|A_{nl}|$, the magnitude of the Zernike moment, can be taken as rotation invariant feature of the underlying image function. Since $A_{n,-l} = A_{nl}^{*}$, then $|A_{n,l}| = |A_{n,-l}|$; thus one can concentrate on $|A_{n,l}|$ with $l \geq 0$ as far as the defined Zernike features are concerned.

2.2.10 Rotational Invariant Features of Complex Moments

As discussed earlier the complex moment of order $(p+q)$ are defined as

$$C_{pq} = \int_{-\infty}^{+\infty} \int_{-\infty}^{+\infty} (x+iy)^p (x-iy)^q f(x,y) dx dy \tag{2.102}$$

Where $p, q = 0, 1, 2, ..., \infty$, and $i = \sqrt{-1}$.

This complex moment is rotationally invariant if $p = q$, so that the angular part can be eliminated. In general the expression $C_{pq}C_{rs}....C_{tu}$ is rotational invariant if only $p + r + ... + t = q + s + ... + u$. As an example the complex moments $C_{11}, C_{22}...., C_{pp}$ are rotational invariant. We know that C_{p0}

and C_{0p} is invariant to Gaussian bluring for $p = 0, 1, 2, ..., \infty$. So it can be proved that $C_{p0}C_{0p}$ is invariant to both Gaussian bluring and rotation for $p = 0, 1, 2, ..., \infty$.

2.3 RESULTS AND DISCUSSION

We have validated the invariant properties of Geometric moments. The translational, scaling and rotational invariance properties have been sucessfully tested for binary images. As mentioned in section 2.2, Geometric central moments are translational invariant. The image shown in Fig. 2.1(a) is letter A and Fig. 2.1(b), (c), (d), (e), (f) and (g) show the image translated to different positions. Because if the translation the centriod of the image changes and given in Table. 2.1. $\overline{x}$ and $\overline{y}$ denotes the centroid of the image in Table 2.1. Central moments computed for these translated images are given in Table. 2.1. For example the moment μ_{20} is constant for all the images which has letter A translated to different positions. As seen from Table. 2.1 other moments such as μ_{02}, μ_{11}, μ_{21}, μ_{12}, μ_{30}, μ_{03} are constant for the translated image. This indicates that although letter A has been translated can be recognised by these moments.

The ratio λ_{pq} that is defined by using central moments as follows has also been found to be scale invariant

$$\lambda_{pq} = \frac{\mu^{'}_{pq}}{(\mu^{'})^{(p+q+2)/2}} = \frac{\mu_{pq}}{\mu^{(p+q+2)/2}}, \quad p+q = 2, 3, ... \tag{2.103}$$

where μ'_{pq} denotes $(p+q)$th order central moment of one image and μ_{pq} denotes $(p+q)$th order central moment of scaled image. μ'_{00} denotes 0th order moment of one image and μ_{00} denotes 0th order moment of scaled image.

Fig. 2.2(a) show the same letter A and the scaled versions are shown in

Fig. 2.2(b) (c) and (d). The object A has been scaled down from as shown in Fig. 2.2(b) to Fig. 2.2(d). The change in moments are very small as given in Table. 2.2. As seen from Table. 2.2, for example λ_{20} changes from 69.973×10^{-5} to 76.906×10^{-5}. Which is very marginal. Similar observations are also made for other moments, such as λ_{20} λ_{11} λ_{21} λ_{12} λ_{30} and λ_{00}. Hence these ratio of moments are scale invariants even though these moments are both scale and translation invariants. This will be an indicator for recognition of objects from different view points or distances.

It is known that Hu's[1] first seven moments are rotational invariant. However, only first three moments ϕ_1, ϕ_2, ϕ_3 are verified. The image considered is shown in Fig. 2.3(a) i.e the letter A. The object i.e. letter A is rotated by 30° each time to obtain the rotated image of Fig. 2.3(b), (c), (d),.....,(l). The image shown in Fig. 2.3(l) correspond to a rotation of 330°. The first three moments computed for each rotation is tabulated in Table. 2.3. It is observed from the Table. 2.3 that there is small variation in the first moment i.e. starting from 122.42 to 132.42. Similarly for ϕ_2 and ϕ_3 also the moment vary within a small range. hence these moments are rotational invariant.

The notion of rotational invariance is also verified for Zernike moments. It is known that magnitude part of the Zernike moments are rotational invariant. We have considered the four lower order moments. i.e. A_{20}, A_{22}, A_{31}, A_{33}. The moments computed for each rotation is tabulated in Table. 2.4. It is observed from Table. 2.4, that the moments A_{20} varies fron 37.32 to 40.59. Which is within a small threshold. The variation for A_{22} is still less. Similar observations are also made for other moments.

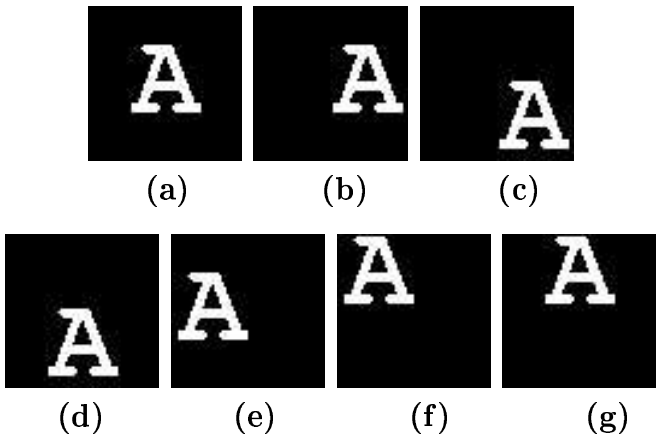

Figure 2.1: Translated images of letter A

	1.1(a)	1.1(b)	1.1(c)	1.1(d)	1.1(e)	1.1(f)	1.1(g)
$\overline{x}$	31	31	46	46	31	16	16
$\overline{y}$	31	46	46	31	16	16	31
μ_{20}	25902	25902	25902	25902	25902	25902	25902
μ_{02}	16894	16894	16894	16894	16894	16894	16894
μ_{11}	2354	2354	2354	2354	2354	2354	2354
μ_{21}	-3224	-3224	-3224	-3224	-3224	-3224	-3224
μ_{12}	88522	88522	88522	88522	88522	88522	88522
μ_{30}	-44492	-44492	-44492	-44492	-44492	-44492	-44492
μ_{03}	43706	43706	43706	43706	43706	43706	43706

Table 2.1: Translation invariance of letter A given in Fig. 2.1 by using translation invariance properties of Geometric moments

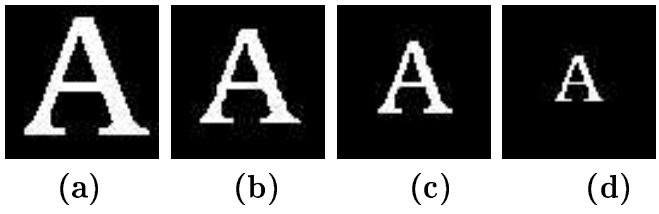

Figure 2.2: Scaled images of letter A

	Fig. 1.2(a)	Fig. 1.2(b)	Fig. 1.2(c)	Fig. 1.2(d)
$\lambda_{20} \times 10^{-5}$	97.226	97.597	99.775	102.451
$\lambda_{02} \times 10^{-5}$	69.973	70.746	71.077	76.906
$\lambda_{11} \times 10^{-5}$	61.445	62.915	60.790	66.31
$\lambda_{21} \times 10^{-5}$	2.180	2.257	2.116	2.378
$\lambda_{12} \times 10^{-5}$	2.052	2.108	2.025	2.234
$\lambda_{30} \times 10^{-5}$	4.010	4.016	4.192	4.272
$\lambda_{03} \times 10^{-5}$	2.486	2.507	2.546	2.761

Table 2.2: Scale invariance of letter A given in Fig. 2.2 by using scale invariance properties of geometric moments

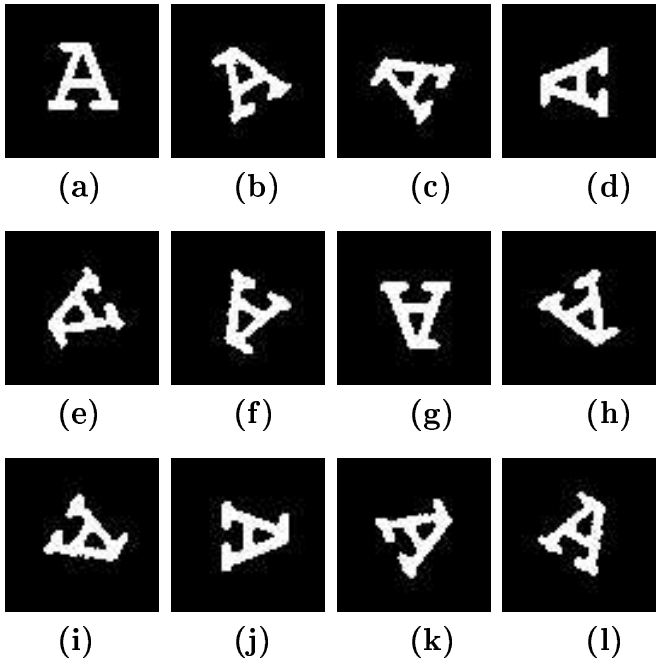

Fig.2.3 Rotated images of letter A

	θ	ϕ_1	ϕ_2	ϕ_3
1.3(a)	0	132.42	9.89	10.43
1.3(b)	30	132.76	9.35	9.48
1.3(c)	60	131.28	11.37	7.87
1.3(d)	90	122.42	7.91	7.86
1.3(e)	120	132.84	6.94	10.04
1.3(f)	150	133.48	10.38	9.39
1.3(g)	180	124.08	8.58	9.63
1.3(h)	210	129.12	8.18	11.78
1.3(i)	240	129.59	9.41	10.28
1.3(j)	270	123.84	7.58	9.87
1.3(k)	300	130.52	8.74	11.66
1.3(l)	330	130.42	9.79	9.94

Table 2.3: Rotational invariance of letter A given in Fig. 2.3 by using the rotational invariance properties of Geometric moments

	θ	$\lvert A_{20}\rvert$	$\lvert A_{22}\rvert$	$\lvert A_{31}\rvert$	$\lvert A_{33}\rvert$
1.3(a)	0	38.41	2.63	23.49	1.01
1.3(b)	30	37.28	2.46	22.46	0.93
1.3(c)	60	37.62	2.48	22.58	0.94
1.3(d)	90	40.73	2.76	24.74	1.06
1.3(e)	120	37.79	2.57	23.10	0.99
1.3(f)	150	37.32	2.56	22.77	0.99
1.3(g)	180	40.43	2.79	24.78	1.08
1.3(h)	210	38.72	2.66	23.74	1.03
1.3(i)	240	37.89	2.59	23.17	0.99
1.3(j)	270	40.59	2.77	24.82	1.06
1.3(k)	300	37.78	2.52	22.83	0.96
1.3(l)	330	37.41	2.46	22.49	0.92

Table 2.4: Rotational invariance of letter A given in Fig. 2.3 by using the rotational invariance properties of Zernike moments

Chapter 3

OBJECT RECOGNITION

Object recognition by image moments has been studies for quite some by many new methodology and strategies[3][4][5][14][13] have been proposed in the literature.In high security Zone, recognation of improtent aspect of identification.Instead of matching the images, its takes large amount of storage space and computational time,becomes a horrendous task. In military appliactions recognition object such as tanks, war plants and other aviation becomes a crutial task. the usual image processing and matching task will take sufficient amount of computational time thus defeating the whole process of recognition. In such situation moment based object recognition will be quite helpful. The invariants properties together with some other approapriet moments could be used for recognition.the challeging task lies when there is subtantial amount of occlusion of the object.In this section ,the issue of moment based object recognition for occluded object is considered.Specifically in outdoor scene consisting of aeroplane flying in open sky may be occluded due to patches of sudden clouds.In an indoor sense, broken bottle may causes hinderance for recognition in case of machine vision systems.A new approach is proposed here for such cases and the limitation also are highlighted.

3.1 NEURAL NETWORK

An Artificial Neural Network (ANN) is an information processing that is inspired by the way biological nervous systems, such as the brain, process information. The key element of this is the novel structure of the information processing system. It is composed of a large number of highly interconnected processing elements (neurones) working in unison to solve specific problems. ANNs, like people, learn by example. An ANN is configured for a specific application, such as pattern recognition or data classification, through a learning process. Learning in biological systems involves adjustments to the synaptic connections that exist between the neurones. This is true of ANNs as well. Neural networks, with their remarkable ability to derive meaning from complicated or imprecise data, can be used to extract patterns and detect trends that are too complex to be noticed by either humans or other computer techniques.Other advantages include:

1. Adaptive learning: An ability to learn how to do tasks based on the data given for training or initial experience.

2. Self-Organisation: An ANN can create its own organisation or representation of the information it receives during learning time.

3. Real Time Operation: ANN computations may be carried out in parallel, and special hardware devices are being designed and manufactured which take advantage of this capability.

4. Fault Tolerance via Redundant Information Coding: Partial destruction of a network leads to the corresponding degradation of performance. However, some network capabilities may be retained even with major network damage.

It is apparent that a neural network devices its computing power through,first,its massively parallel distributed structure and,second,its ability to learn and therefore generalize.Generalization refers to the neural network producing reasonable outputs for inputs not encountered during training (learning).These two information-processing capabilities make it possible for neural networks to solve complex problem.

3.1.1 Network Architechtures

The manner in which the neuron of a neural network are structure is intimately link with a learning used to train the network. We may therefor speak of learning algorithm used in the design of neural network as been structured.

3.1.2 Single-Layer Feedforward Networks

Feed-forward ANNs allow signals to travel one way only; from input to output. There is no feedback (loops) i.e. the output of any layer does not affect that same layer. Feed-forward ANNs tend to be straight forward networks that associate inputs with outputs. They are extensively used in pattern recognition. This type of organisation is also referred to as bottom-up or top-down.

3.1.3 Multilayer Feedforwad Networks

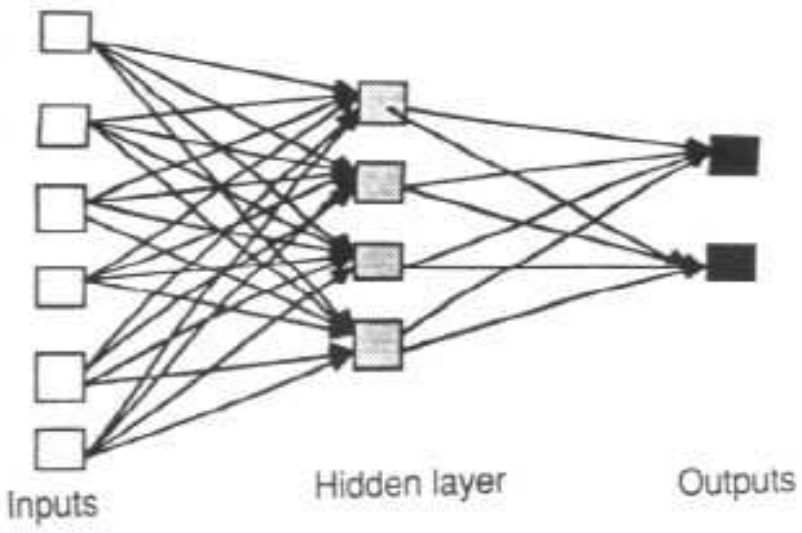

(a)

Figure 3.1: Schamatic diagram of typical a multilayer feedforward network

This class of a feedforward neural network distinguises by its self by the presence of one or more hidden layers,whose computation nodes are correspondingly called hidden neurons or hidden units.The function of hidden neurons is to intervene between the external input and the network output in some useful manner .By adding one or more hidden layers,the network is enabled to extact higher-order statistics.The ability of hidden neurons to extract higher-order statistic is particularly valuable when the size of the input layer is large. The backpropagation[17] algorithm is used to train a given feed-forward multilayer neural network for a given set of input patterns with known classifications. When each entry of the sample set is presented to the network, the network examines its output response to the sample input pattern. The output response is then compared to the known and desired output and the error value is calculated. Based on the error, the connection weights are adjusted. The backpropagation algorithm is based on Widrow-Hoff delta learning rule in which the weight adjustment is done through mean square error of the output response to the sample input. The set of these sample patterns are repeatedly presented to the network until the error value is minimized. Now Fig(3.1) presents the architectural layout of a multilayer perceptron .The sequential updating of weights is the preffered method for online implementation of the back propagation algorithm.For this mode of operation,the algorithm cycles through the training sample $\{(X(n), d(n))\}_{n=1}^{N}$ as follows:

1.*Initialization.* Assuming that no prior information is available,pick the synaptic weight and thresholds from a uniform distribution whose mean is zero and whose variance is chosen to make the standard deviation of the induced local fields of the neurons lie at the transition between the linear and satuareted parts of the sigmoid activation function.

2.*Presentations and Training Examples.* Present the network with an epoch of training examples.For each example in the set ,ordered in some fashion ,perform the sequence of forward and backward computations describe under points 3 and 4 , respectively.

3.*Forward Computation.* Let a training example in the epoch be denoted by $(X(n), d(n))$, with the input vector $x(n)$ applied to the input layer of sensory nodes and the desired response vector $d(n)$ presented to the output layer of computation nodes .Compute the induced local fields and function signals of the network by proceding forward through the network , layer by layer. The induced local field $v_j^{(\ell)}(n)$ for neuron j in layer ℓ is

$$v_j^{(l)}(n) = \sum_{i=0}^{m_0} \omega_{ji}^{(l)}(n)\, y_i^{(l-1)}(n) \tag{3.1}$$

where $y_i^{(l-1)}(n)$ is the output(function) signal of neuron i in the previous layer $l-1$ at iteration n and $\omega_{ji}^{(l)}(n)$ is the synaptic weight of neuron j in layer l that is fed from neuron i in the layer $l-1$ .For $i=0$,we have $y_0^{(l-1)}(n) = +1$ and $\omega_{j0}^{(n)} = b_j^{(l)}(n)$ is the bias applied to neuron j in layer j.Assuming the use of a sigmoid function ,the output signal of neuron j in layer l is

$$y_j^{(l)} = \varphi_j(v_j(n)) \tag{3.2}$$

If neuron j is in the first hidden layer $(i.e, \ell = 1)$, set

$$y_j^{(0)}(n) = x_j(n) \tag{3.3}$$

where $x_j(n)$ is the jth element of the input vector $x(n)$.If neuron j is in the output layer (i.e,l=L, where L is reffered to as the depth of the network), set

$$y_j^L = o_j^{(n)} \tag{3.4}$$

Compute the error signal

$$e_j(n) = d_j(n) - o_j(n) \tag{3.5}$$

where $d_j(n)$ is the jth element of the desired response vector $d(n)$.

4.*Backward Computation.*Compute the δs(i.e,local gradients) of the network ,defined by

$$\delta_j^{(l)}(n) = \begin{cases} e_j^{(L)}(n)\varphi_j'(v_j^{(L)}(n)) & for\ neuron\ \text{j}\ in\ output\ layer\ \text{L} \\ \varphi_j'(v_j^{(n)}(n))\sum_k \delta_k^{(l+1)}(n)\omega_{kj}^{(l+1}(n) & for\ neuron\ \text{j}\ in\ hidden\ layer\ \text{l} \end{cases} \tag{3.6}$$

where the prime in $\varphi_j^{'}(.)$ denotes differentiation with respect to the argument. adjust the synaptic weights of the network in layer l according to the generalized delta rule:

$$\omega_{ji}^{(l)}(n+1) = \omega_{ji}^{(l)}(n) + \alpha[\omega_{ji}^{(l)}(n-1)] + \eta\delta_j^{(l)}(n)y_i^{(l-1)}(n) \tag{3.7}$$

where η is the learning rate parameter and α is the momentum constant.

5.*Iteration.*Iterate the forward and backward computation under points 3 and 4 by presenting new epochs of training examples to the network until the stopping criterion is met.

3.2 RECOGNITION

We considered two typical cases one outdoor and one indoor cases. In particular we addressed the issue of object recognition with occlusion of different part of the object .Since, concern is to recognised the object and try for exact reconstruction, some lower order moments that is viewed to represent the smooth part and less edges are considered. In case of machine vision system the object may here translation, rotation and scalling.Geometric moments are possces invariants the properties.In this consider,some translation invariants moments together with lower order moments for recognition in case of machine vision systems.

When an object is occluded,the moments will change.The following Schemes is adopted for such a process.The inputs consists of translational invariants moments and some lower order moments.

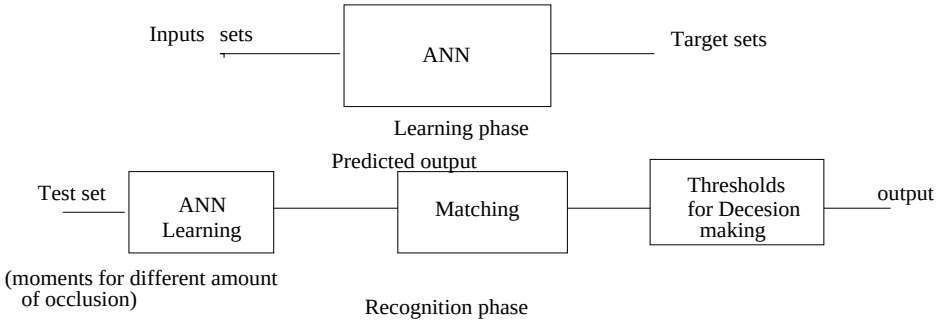

(a)

Figure 3.2: Block diagram of recognition

We have consider ten such moments upto third order.Moments set with different amounts of occlusion of the object are computed.These set of moments from the inputs tranning set for a Artificial Neural Network.The target set consists of the moments of the objects.The ANN,consider is a feedforward multilayered network.The ANN is trained with these training set using Back-propagation(BP)learning algorithm .This is demostrated in Fig.3.2.Onece the network is trained with the data set,the weights are freezed and used for the prediction.Difference set of moments for a wide variety of occlusion have been computed and are used as the input sets.The target set is stored and predicted moments is matched with the store moments for decesion making of the object.the output is either the systems recognises or fails.This is shown in Fig.3.2.Particularly, we have investigated with specific situation that is aeroplane flying or indoor object.However,this Scheme can be extended for wide class of object whose moments are with in a certain threshold.

3.3 RESULTS AND DISCUSSION

In simulation, real as well as binary images are consider.One indoor,Two outdoor or one binary outdoor image is considered.Fig3.4(a) shows the indoor image consisting of a bottle.Different occluded version are created and are shown in Fig.3.4(b,c,d,e,f).Ten lower order geometric moments for each occluded object is computed and these five training sets are formed.The target set correponds to the respective moments of the original image as shown in Fig.3.4(a).The training set is tabulated in table(3.1).The ANN consists of ten inputs neurons ,five hidden neurons and ten outputs neurons.The activation function use is the sigmoidal function and the slope $\lambda = 0.1$ .The learning rate η of the BP algorithm is fixed at 0.4.The learning curve is shown in Fig.3.3(a) where the network is trained after 50 to 100 interation.This could be due to less amount of occlusion of the object.The test sets of images are in shown in Fig3.5.The corresponding prediction and Percentage prediction error are tabulated in table 3.2 and table 3.3.For occulasion of different portion of the object,the prediction error is within 0.25(%) and hence matching followed by recognition is possible.For quite a different object that is aeroplane in the sky,the error are quite large as tabulated in table 3.3. The second set of training images are shown in Fig.3.6,different amount of occlusion.The normalised training set is provided in table 3.4. The ANN topology remains same as the previous example.The network is trained and the learning curve is shown in Fig.3.3(b).The test set of images are shown in Fig.3.7.The predicted output and the percentage of error are tabulated in table.3.5,table.3.6 and table.3.7.It is observed that for a wide variety of occlusion ,the prediction error is very less while the object changed,the error is quite large that differentiating one object from other.

The third set of training images at the set of aeroplane images as shown in

Fig.3.9. The corresponding moments are given in table.3.8. The training set includes different amount of occlusion. The test set of images are shown in Fig.3.10 and Fig.3.11. For the images shown in Fig.3.10, the prediction error is very large for the test images of Fig.3.11. Thus for different images the network fails. this also visually true as observed from Fig.3.11(a) and Fig.3.11(b). Binary images of aeroplane are also considered for training the network. The training set is presented in table 3.12 . There are occlusion in different portion of the image. For the test images shown in Fig3.13(a) and Fig.3.13(b). The prediction error is within threshold and for Fig.3.13(c) and Fig.3.13(d) the error is very large and hence fault to recognised the object. The prediction error are tabulated in tabe 3.14.

It is observed , that for different amount of occlusions , the network would be recognize the object while beyond certain portion of occlusions, The network fails .

Moments	Fig.3.4(b)	Fig.3.4(c)	Fig.3.4(d)	Fig.3.4(e)	Fig.3.4(f)
μ_{00}	0.000395997	0.000396022	0.000400603	0.000398358	0.000395937
μ_{10}	0.018908862	0.018891382	0.019245777	0.019149784	0.018935144
μ_{01}	0.020193356	0.020196084	0.020425924	0.020314765	0.020188507
μ_{20}	0.333060819	0.333778301	0.335079324	0.335369647	0.332788623
μ_{02}	0.337588445	0.337601938	0.337620544	0.337620718	0.337679613
μ_{11}	0.001794388	0.0018751	0.001172884	0.001042956	0.001572844
μ_{30}	0.014393618	1.000000000	0.108532159	0.110830607	0.020512623
μ_{12}	0.428192875	0.427701665	0.09123853	0.091992131	0.428940545
μ_{21}	0.313142537	0.309282165	0.311471909	0.307545466	0.315146345
μ_{03}	0.670367549	0.670416142	0.67023937	0.670341741	0.669774382

Table 3.1: Inputs moments of bottle

Moments	Target	Fig.3.5(a)		Fig.3.5(b)	
		Prediction	Error(%)	Prediction	Error(%)
μ_{00}	0.000394482	0.000402	2.03	0.000375	4.82
μ_{10}	0.018858878	0.019043	0.98	0.018407	2.39
μ_{01}	0.020128074	0.020320	0.95	0.019656	2.34
μ_{20}	0.332729498	0.333087	0.10	0.331819	0.27
μ_{02}	0.337162876	0.337507	0.01	0.336284	0.26
μ_{11}	0.001320147	0.001342	0.00	0.001265	4.17
μ_{30}	0.020035019	0.020227	0.95	0.019563	2.35
μ_{12}	0.425431293	0.425603	0.04	0.424991	0.10
μ_{21}	0.990872375	0.990765	0.01	0.991136	0.02
μ_{03}	0.666641673	0.666290	0.05	0.667538	0.13

Table 3.2: Prediction and percentage of error of test images

Moments	Target	Fig.3.5(c)		Fig.3.5(d)	
		Prediction	Error(%)	Prediction	Error(%)
μ_{00}	0.000394482	0.000393	0.25	0.000433	9.89
μ_{10}	0.018858878	0.018837	0.11	0.019740	4.67
μ_{01}	0.020128074	0.020105	0.11	0.021048	4.57
μ_{20}	0.332729498	0.332680	0.01	0.334433	0.51
μ_{02}	0.337162876	0.337115	0.01	0.338806	0.48
μ_{11}	0.001320147	0.001317	0.22	0.001429	8.25
μ_{30}	0.020035019	0.020012	0.11	0.020955	4.59
μ_{12}	0.425431293	0.425407	0.00	0.426252	0.19
μ_{21}	0.990872375	0.990885	0.00	0.990355	0.05
μ_{03}	0.666641673	0.666690	0.00	0.664965	0.25

Table 3.3: Prediction and percentage of error of test images

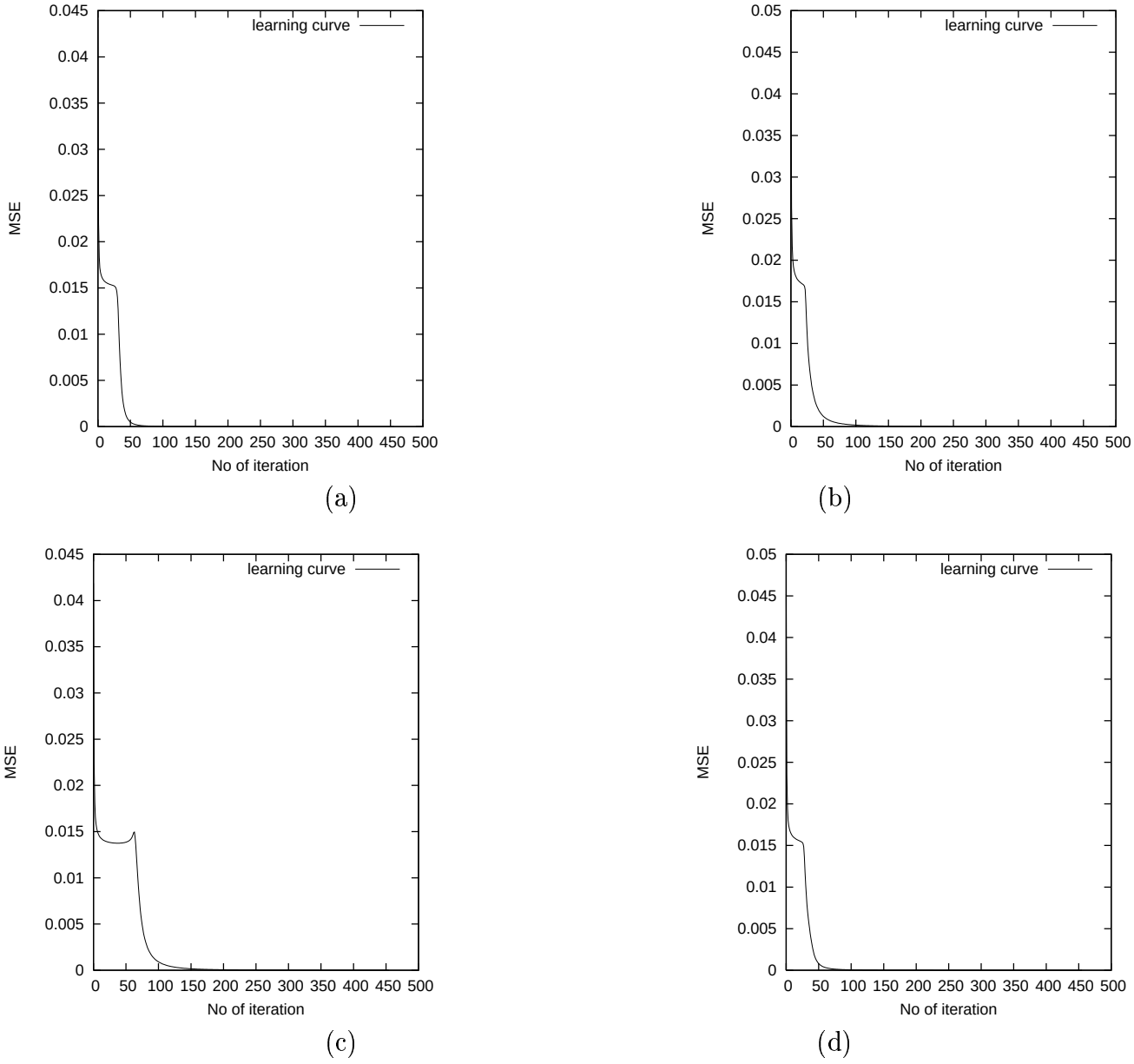

Figure 3.3: Learning curve of different test images

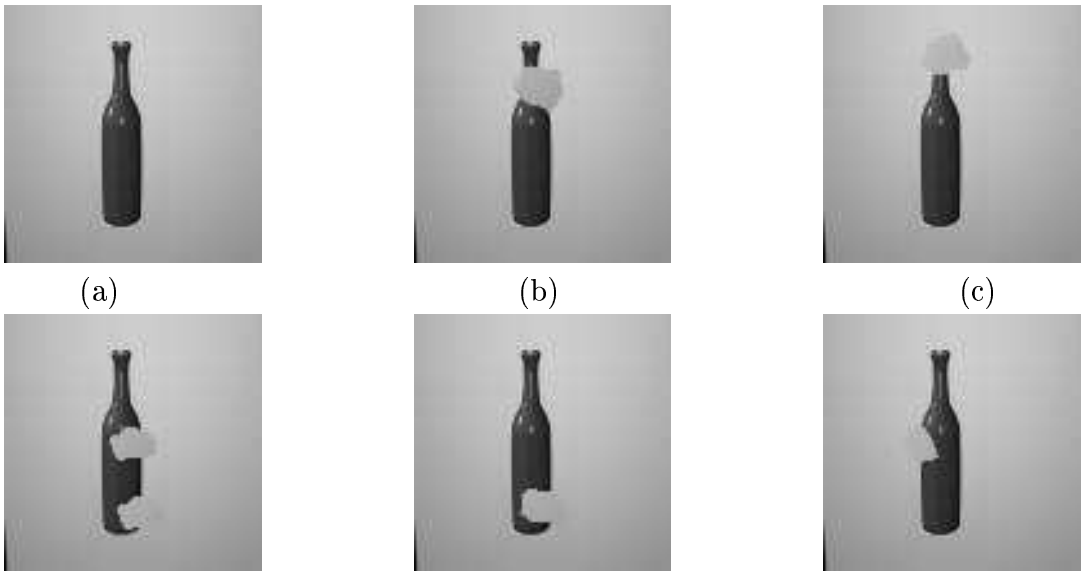

(a) (b) (c)

(d) (e) (f)

Figure 3.4: Training set of images

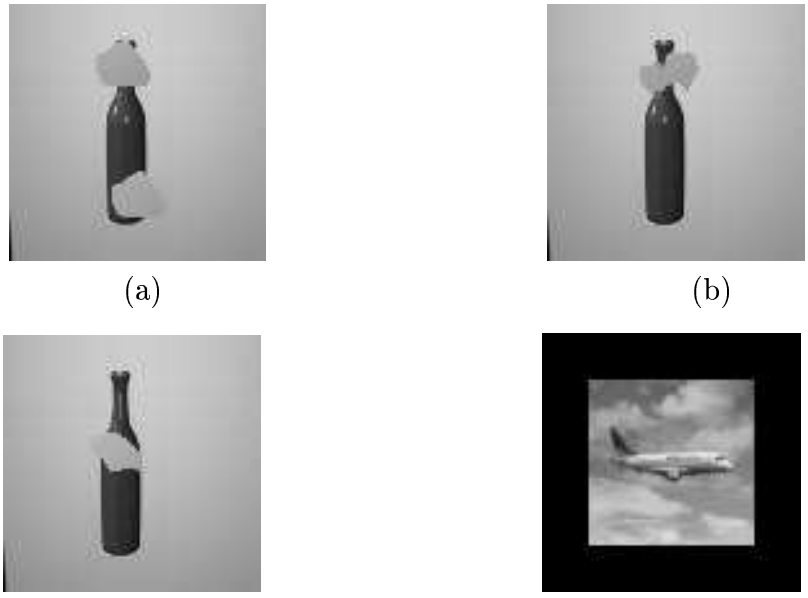

(a) (b)

(c) (d)

Figure 3.5: Test set of images

Moments	Fig.3.6(b)	Fig.3.6(c)	Fig.3.6(d)	Fig.3.6(e)	Fig.3.6(f)
μ_{00}	0.00021875	0.000220553	0.000218953	0.000219771	0.000211147
μ_{10}	0.010767352	0.010998742	0.010853392	0.010863965	0.010304975
μ_{01}	0.011120432	0.011454806	0.011526242	0.011475357	0.010926435
μ_{20}	0.190612938	0.194260108	0.193311535	0.192205209	0.190045758
μ_{02}	0.169602901	0.176296987	0.169974077	0.174413908	0.173114137
μ_{11}	0.983961389	0.988992659	0.991157803	0.990781482	0.989262468
μ_{30}	0.979149889	0.072832424	0.057729102	0.027247133	0.556803279
μ_{12}	0.732884237	0.945165459	0.889121823	0.928803705	0.051437744
μ_{21}	0.443211277	0.380573048	0.219920424	0.227933159	0.364586389
μ_{03}	0.5570663	0.307161857	1.000000000	0.822046491	0.317576971

Table 3.4: input car moment

Moments	Target	Fig.3.7(a)		Fig.3.7(b)	
		Prediction	Error(%)	Prediction	Error(%)
μ_{00}	0.000224756	0.000225	0.44	0.000221	1.33
μ_{10}	0.011207859	0.011201	0.05	0.011104	0.91
μ_{01}	0.01163371	0.011627	0.05	0.011527	0.91
μ_{20}	0.194294363	0.194252	0.02	0.193832	0.23
μ_{02}	0.176668947	0.176628	0.02	0.176208	0.26
μ_{11}	0.98896782	0.988974	0.00	0.989070	0.01
μ_{30}	0.073077202	0.073052	0.03	0.072720	0.48
μ_{12}	0.945358454	0.945379	0.00	0.945663	0.03
μ_{21}	0.380255451	0.380230	0.00	0.380019	0.06
μ_{03}	0.302836943	0.302799	0.01	0.302465	0.12

Table 3.5: Prediction and percentage of error of test images

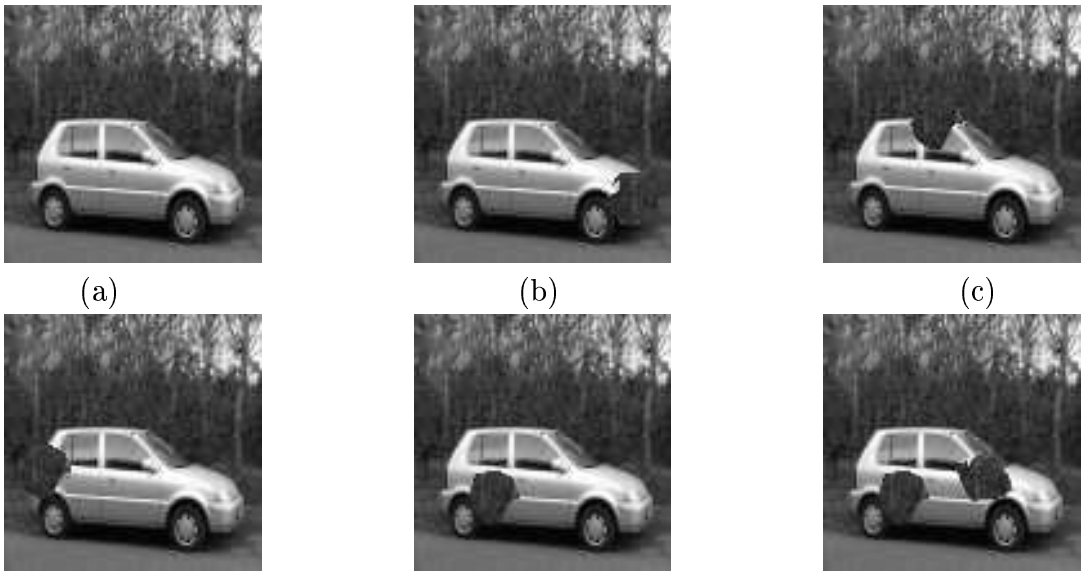

(a) (b) (c)

(d) (e) (f)

Figure 3.6: Training set of images

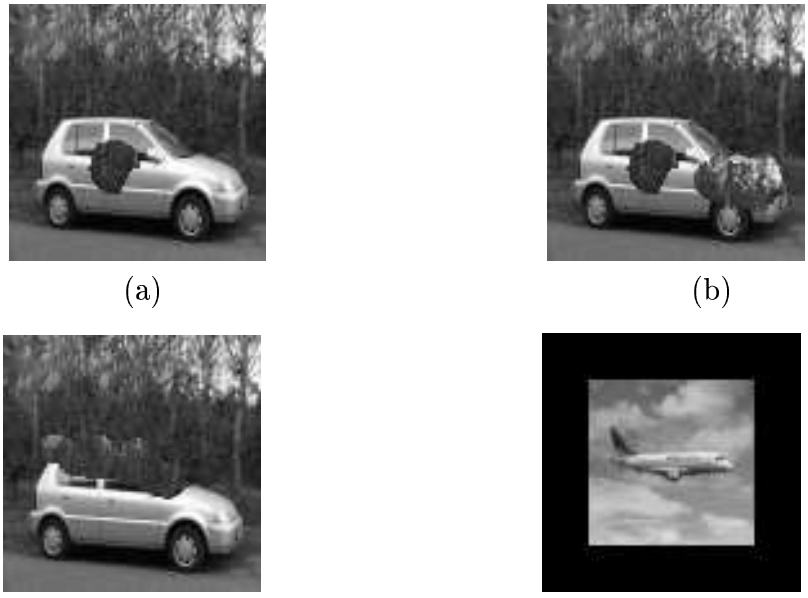

(a) (b)

(c) (d)

Figure 3.7: Test set of images

Moments	Target	Fig.3.7(c)		Fig.3.7(d)	
		Prediction	Error(%)	Prediction	Error(%)
μ_{00}	0.000224756	0.000225	0.13	0.000232	3.57
μ_{10}	0.011207859	0.011200	0.06	0.011380	1.54
μ_{01}	0.01163371	0.011626	0.06	0.011810	1.52
μ_{20}	0.194294363	0.194247	0.02	0.195015	1.90
μ_{02}	0.176668947	0.176623	0.02	0.177392	0.40
μ_{11}	0.98896782	0.988975	0.00	0.988798	0.01
μ_{30}	0.073077202	0.073048	0.03	0.073657	0.79
μ_{12}	0.945358454	0.945383	0.00	0.944862	0.05
μ_{21}	0.380255451	0.380227	0.00	0.380612	0.09
μ_{03}	0.302836943	0.302795	0.01	0.303403	0.18

Table 3.6: Prediction and percentage of error of test images

(a) **(b)**

Figure 3.8: Test set of images

Moments	Target	Fig.3.8(a)		Fig.3.8(b)	
		Prediction	Error(%)	Prediction	Error(%)
μ_{00}	0.000224756	0.000227	1.33	0.000224	0.00
μ_{10}	0.011207859	0.011269	0.55	0.011180	0.24
μ_{01}	0.01163371	0.011696	0.54	0.011605	0.24
μ_{20}	0.194294363	0.194541	0.12	0.194160	0.06
μ_{02}	0.176668947	0.176917	0.14	0.176535	0.07
μ_{11}	0.98896782	0.988908	0.00	0.988996	0.00
μ_{30}	0.073077202	0.073280	0.27	0.072978	0.13
μ_{12}	0.945358454	0.945184	0.01	0.945442	0.00
μ_{21}	0.380255451	0.380374	0.03	0.380183	0.01
μ_{03}	0.302836943	0.303027	0.06	0.302725	0.03

Table 3.7: Prediction and percentage of error of test images

Moments	Fig.3.9(b)	Fig.3.9(c)	Fig.3.9(d)	Fig.3.9(e)	Fig.3.9(f)
μ_{00}	0.000147829	0.000147211	0.000147706	0.00014816	0.000147064
μ_{10}	0.007753164	0.007717136	0.00774841	0.007746076	0.007703335
μ_{01}	0.007537576	0.007487081	0.007501113	0.007486512	0.007468541
μ_{20}	0.050640543	0.050630273	0.050652235	0.0508578	0.050680295
μ_{02}	0.049601456	0.049147311	0.049073046	0.049857249	0.049063181
μ_{11}	1.000072957	1.000001611	1.000001756	1.000425006	1.000017714
μ_{30}	0.972458709	0.972394909	0.972533954	0.969734201	0.971943293
μ_{12}	0.04452373	0.043014379	0.043071725	0.03391268	0.04282493
μ_{21}	0.047560659	0.04730305	0.047313641	0.042453009	0.04712503
μ_{03}	0.092450584	0.082267779	0.080917277	0.063360991	0.08090235

Table 3.8: Inputs moments of aeroplane

Moments	Target	Fig.3.10(a)		Fig.3.10(b)	
		Prediction	Error(%)	Prediction	Error(%)
μ_{00}	0.000146244	0.000150	2.73	0.000150	2.73
μ_{10}	0.007667079	0.007667	0.00	0.007667	0.00
μ_{01}	0.007429526	0.007429	0.00	0.007429	0.00
μ_{20}	0.050627434	0.050627	0.00	0.050627	0.00
μ_{02}	0.049043626	0.049043	0.00	0.049043	0.00
μ_{11}	1.000000000	0.999961	0.00	0.999961	0.00
μ_{30}	0.972402349	0.972403	0.00	0.972403	0.00
μ_{12}	0.042975071	0.042974	0.00	0.042974	0.00
μ_{21}	0.047281415	0.047281	0.00	0.047281	0.00
μ_{03}	0.081013108	0.081012	0.00	0.081012	0.00

Table 3.9: Prediction and percentage of error of test images

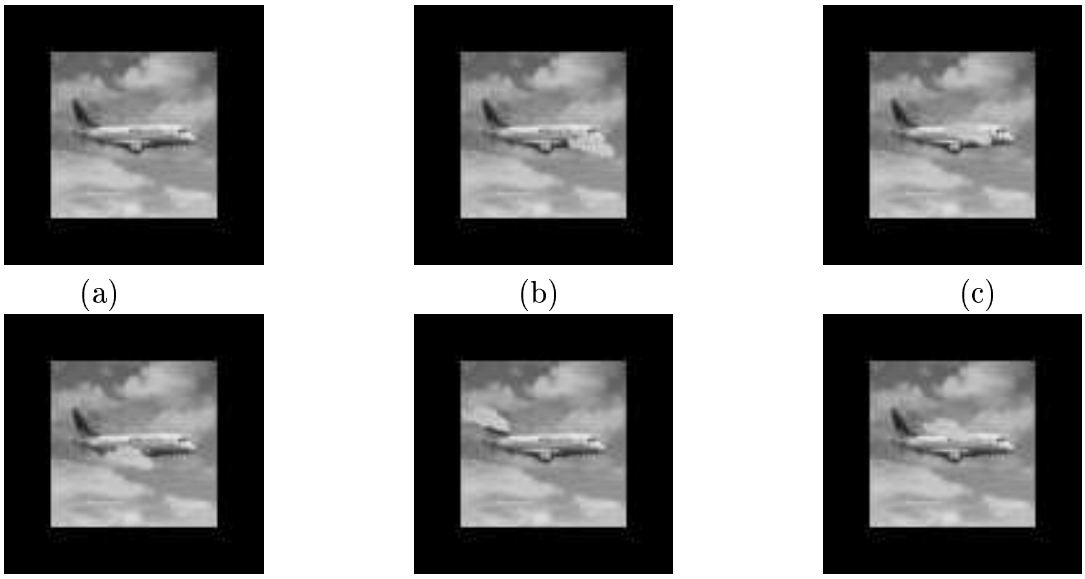

Figure 3.9: Training set of images

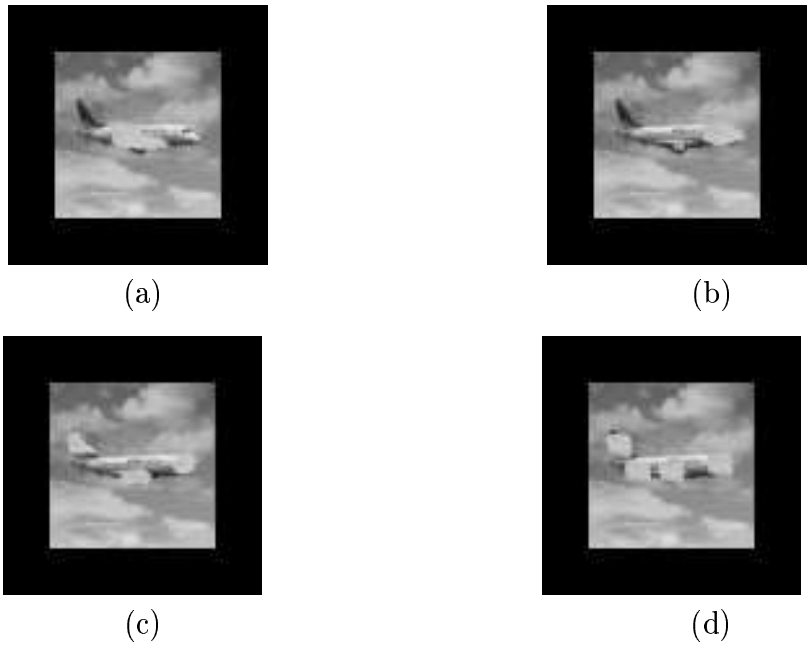

Figure 3.10: Test set of images

Moments	Target	Fig.3.10(c)		Fig.3.10(d)	
		Prediction	Error(%)	Prediction	Error(%)
μ_{00}	0.000146244	0.000150	2.73	0.000150	2.73
μ_{10}	0.007667079	0.007667	0.00	0.007667	0.00
μ_{01}	0.007429526	0.007430	0.01	0.007430	0.00
μ_{20}	0.050627434	0.050628	0.00	0.050629	0.00
μ_{02}	0.049043626	0.049045	0.00	0.049045	0.00
μ_{11}	1.000000000	0.999961	0.00	0.999961	0.00
μ_{30}	0.972402349	0.972402	0.00	0.972402	0.00
μ_{12}	0.042975071	0.042976	0.00	0.042976	0.00
μ_{21}	0.047281415	0.047282	0.00	0.047283	0.00
μ_{03}	0.081013108	0.081014	0.00	0.081015	0.00

Table 3.10: Prediction and percentage of error of test images

(a) **(b)**

Figure 3.11: Test set of images

Moments	Target	Fig.3.11(a)		Fig.3.11(b)	
		Prediction	Error(%)	Prediction	Error(%)
μ_{00}	0.000146244	0.000334	128	0.000172	17.80
μ_{10}	0.007667079	0.011832	54.32	0.008255	7.66
μ_{01}	0.007429526	0.011488	54.63	0.008002	7.71
μ_{20}	0.050627434	0.064668	27.73	0.052791	4.27
μ_{02}	0.049043626	0.062805	28.06	0.051161	4.31
μ_{11}	1.000000000	0.999900	0.01	0.999954	0.00
μ_{30}	0.972402349	0.962519	1.01	0.970923	0.15
μ_{12}	0.042975071	0.055866	29.99	0.044945	4.58
μ_{21}	0.047281415	0.060788	28.56	0.049356	4.38
μ_{03}	0.081013108	0.098528	21.61	0.083775	3.40

Table 3.11: Prediction and percentage of error of test images

Moments	Fig.3.12(b)	Fig.3.12(c)	Fig.3.12(d)	Fig.3.12(e)	Fig.3.12(f)
μ_{00}	0.000486819	0.000494959	0.000487285	0.000488067	0.000489806
μ_{10}	0.024574799	0.024976417	0.024266027	0.024993421	0.024726304
μ_{01}	0.025087143	0.025337473	0.02475833	0.024800148	0.024455426
μ_{20}	0.451406978	0.451753778	0.462315353	0.462718151	0.451535043
μ_{02}	0.45823772	0.444546248	0.442754733	0.442771285	0.458091006
μ_{11}	0.000052721	1.001925928	0.000708135	1.001605701	0.000160503
μ_{30}	0.675796736	0.675763599	0.703762803	0.701237918	0.676052448
μ_{12}	0.232199241	0.224761107	0.662804867	0.246149472	0.231100849
μ_{21}	0.889691452	0.891126675	0.330571813	0.332306867	0.78181702
μ_{03}	0.291563963	0.795503546	0.0862587	0.086386952	0.924974338

Table 3.12: Inputs moments of binary aeroplane

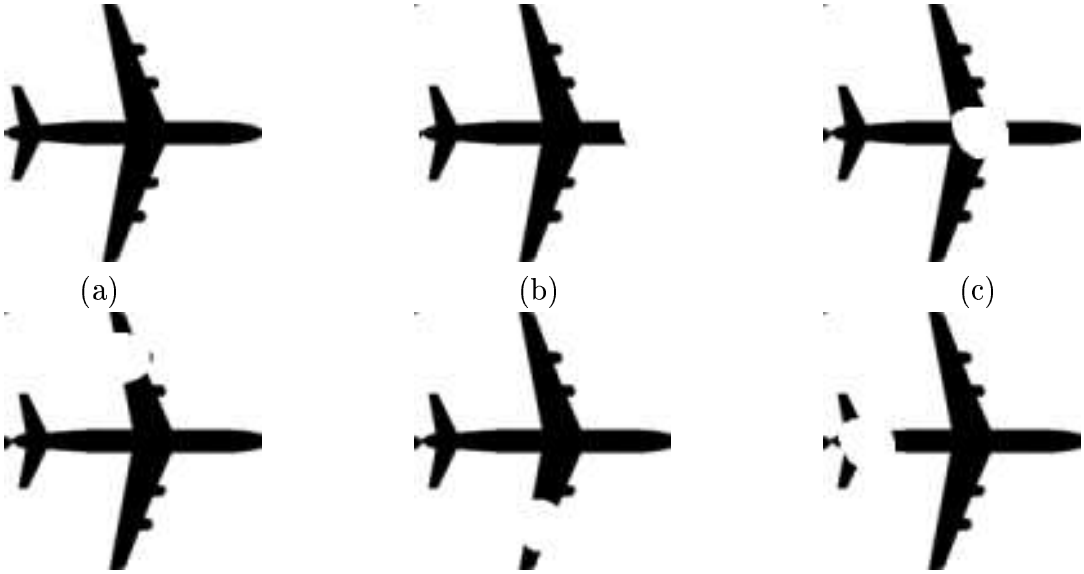

Figure 3.12: Training set of images

Moments	Target	Fig.3.13(a)		Fig.3.13(b)	
		Prediction	Error(%)	Prediction	Error(%)
μ_{00}	0.000477048	0.000474	0.62	0.000508	6.49
μ_{10}	0.024079478	0.024008	0.29	0.024793	2.96
μ_{01}	0.024497701	0.024426	0.28	0.025218	2.94
μ_{20}	0.451464339	0.451425	0.00	0.451834	0.08
μ_{02}	0.440715875	0.440670	0.01	0.441149	0.09
μ_{11}	0.000166977	0.000168	1.20	0.000182	9.63
μ_{30}	0.66984873	0.669973	0.00	0.668660	0.17
μ_{12}	0.217559591	0.217382	0.08	0.219269	0.78
μ_{21}	1.000000000	0.999961	0.00	0.999957	0.00
μ_{03}	0.027764911	0.027686	0.28	0.028551	2.83

Table 3.13: Prediction and percentage of error of test images

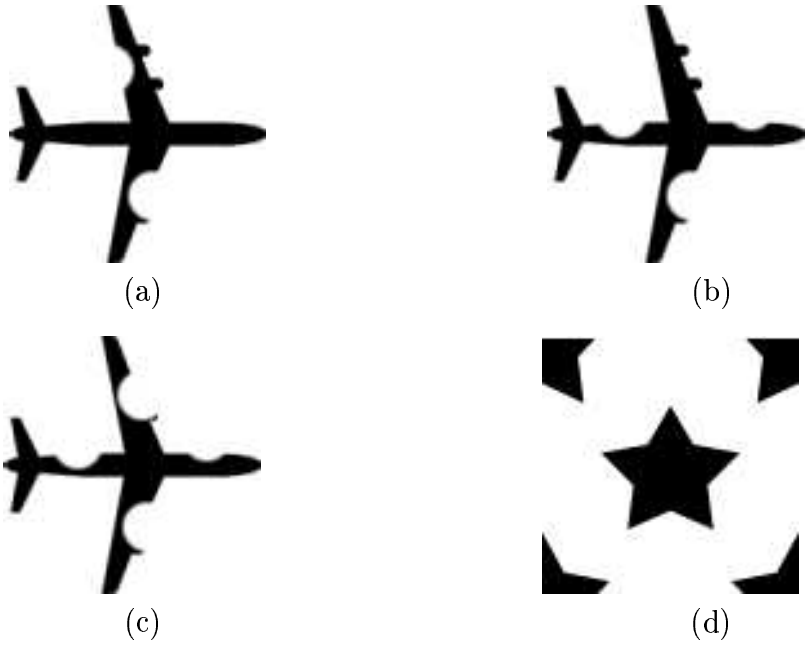

(a) (b)

(c) (d)

Figure 3.13: Test set of images

Moments	Target	Fig.3.13(c)		Fig.3.13(d)	
		Prediction	Error(%)	Prediction	Error(%)
μ_{00}	0.000477048	0.000521	9.22	0.000509	6.70
μ_{10}	0.024079478	0.025081	4.15	0.024812	3.04
μ_{01}	0.024497701	0.025508	4.12	0.025237	3.02
μ_{20}	0.451464339	0.451980	0.11	0.451844	0.08
μ_{02}	0.440715875	0.441321	0.13	0.441160	0.10
μ_{11}	0.000166977	0.000187	12.6	0.000182	9.63
μ_{30}	0.66984873	0.668188	0.24	0.668629	0.18
μ_{12}	0.217559591	0.219949	1.09	0.219315	0.80
μ_{21}	1.000000000	0.999956	0.00	0.999957	0.00
μ_{03}	0.027764911	0.028867	3.97	0.028572	2.90

Table 3.14: Prediction and percentage of error of test images

Chapter 4

RECONSTRUCTION USING ZERNIKE AND PSEUDO-ZERNIKE MOMENTS

Moment function are used in several computer vision and related application such as pattern recognition, object identification,template matching and pose estimation.Zernike,pseudo-Zernike moment use continuos orthogal polynomials as basis function and its give better feature represent capability .But different type of other moments also have used for recostruction purpose. different authors have been propose different method and algorithm for computational and minimum error.R.mukundan[15] have proposed discrete orthogonal moments that have several computational advantage over continuous moments.In another paper Mukundan[16] proposed radial Tchebichef moments.This moments have a radial -polar form similar to Zernike moments. The first significant work considering moments for patter recognition was performed by Hu[1]. The completeness of their description results in one of their often cited attributes, the ability to reconstruct an object from its set of moments. It is quite difficult to reconstruct of an image from non

orthogonal moments, as their kernel functions are not orthogonal.

There are two methods to reconstruct an image from non orthogonal geometric moments.One is moment matching method and another is Fourier transform method.In moment matching method, derives a contineous function.

$$g(x,y) = g_{00} + g_{10}x + g_{01}y + g_{20}x^2 + g_{11}xy + g_{02}y^2 + ... \qquad (4.1)$$

Whose moments exactly match the moments, $\{m_{pq}\}$ of $f(x,y)$ through order N_{max}. However, this method is shown to be impractical as it requires the solution to an increasing number of coupled equations as higher order moments are considered.In fourier transform method, as kernels are not orthogonal it requires more number of moments for reconstruction. The reconstruction of an image from complex moments is also quite difficult.

Image can be reconstructed easily from a set of orthogonal moments, such as Legendre, Zernike[7] and Pseudo-Zernike moments. As their kernel functions are orthogonal, it require less number of moments than that of non orthogonal moments. The orthogonal moments are better than the other types of moments in terms of information redundancy. Performance of Zernike and Pseudo-Zernike moments are better in presence of noise[6], but the main problen is co compute the radial polynomials, which takes long computation time to derive the Zernike and Pseudo-Zernike moments.

Since the contineous orthogonal moments are defined only inside a limit domain([-1,1] for Legendre moments and the unit circle for the case of Zernike and Pseudo-Zernike moments), the computation of those required a coordinate transformation. Another problem with the aforementioned moment is approximation of contineous integral, which not only leads to numerical errors but also severely affects the analytical properties which they were intended it satisfy, such as invariance and orthogonality.

4.1 RECONSTRUCTION USING ZERNIKE MOMENTS

Zernike function introduced by Frits Zernike, a Dutch mathematician and physician, is a set of complex orthogonal functions with asimple rotational property which forms a complete orthogonal basis over the class of square integrable functions defined over the unit disk. The kernel of Zernike moments is the orthogonal Zernike polynomials defined over polar coordinates inside a unit circle[7]. The two-dimentional Zernike moments of order p with repetition q of an image intensity function $f(r,\theta)$ are defined as follow.

$$Z_{pq} = \frac{p+1}{\pi} \int_0^1 \int_{-\pi}^{\pi} [V_{pq}(r,\theta)]^*.f(r,\theta) r \; dr \; d\theta \tag{4.2}$$

where $r < 1$ and $x^2 + y^2 \leq 1$. The Zernike polynomials $V_{pq}(r,\theta)$ of order p are defined as

$$V_{pq}(r,\theta) = R_{pq}(r) e^{jq\theta} \tag{4.3}$$

and its real valued radial polynomial is given by

$$R_{pq}(r) = \sum_{s=0}^{\frac{(p-|q|)}{2}} (-1)^s . \frac{(p-s)!}{s!(\frac{p+|q|}{2}-s)!(\frac{p-|q|}{2}-s)!} r^{p-2s} = \sum_{\substack{k=|q| \\ p-|q|=even}}^{p} B_{p|q|k} r^k \tag{4.4}$$

where $0 \leq |q| \leq p$ and $p \geq 0$. the orthogonal Zernike polynomials satisfy the following condition

$$\frac{p+1}{\pi} \int_0^1 \int_{-\pi}^{\pi} [V_{pq}(r,\theta)][V_{mn}(r,\theta)]^*.f(r,\theta) r \; dr \; d\theta$$

$$= \begin{cases} \frac{\pi}{p+1} \delta_{pn} \delta_{qm} & if \; p = n, \;\; q = m \\ 0 & otherwise \end{cases} \tag{4.5}$$

The radial function also satisfy the orthogonality relation

$$\int_0^1 [R_{pq}(r,\theta)][R_{mn}(r,\theta)]^* r \; dr \; d\theta = \frac{1}{2(p+1)}\delta_{pn} \tag{4.6}$$

where δ_{ij} is the Kronecker delta. The discrete approximation of Zernike moments is expressed as follow

$$Z_{pq} = \sum_x \sum_y \tau_p R_{pq}(r) e^{-jq\theta} f(r,\theta) \tag{4.7}$$

where τ_p is the normalizing constant based on the mapping transformation.

Since Zernike moments are defined in terms of polar coordinates (r,θ) with $|r| \leq 1$, the computation of Zernike polynomials requires a linear transformation of the image coordinates (i,j), $i,j = 0,1,2,.....,N-1$ to a suitable domain $(x,y) \in R^2$ inside a unit circle. Two commonly used cases of the the transformations are shown in Fig. 4.1(b) and 4.1(c). Based on these figures, we have the following discrete approximation of the contineous Zernike moments' integral in Eq(4.2):

$$Z_{pq} = \lambda(p,N) \sum_{i=0}^{N-1} \sum_{j=0}^{N-1} R_{pq}(r_{ij}) e^{-jq\theta_{ij}} f(i,j), \qquad 0 \leq r_{ij} \leq 1 \tag{4.8}$$

where the most general image coordinate transformation to the interior of the unit circle is given by

$$r = \sqrt{(c_1 i + c_2)^2 + (c_1 j + c_2)^2} \tag{4.9}$$

$$\theta = tan^{-1}\left(\frac{c_1 j + c_2}{c_1 i + c_2}\right) \tag{4.10}$$

In particular, for Fig. 4.1(b)

$$\lambda(p,N) = \frac{p+1}{(N-1)^2}, \quad c_1 = \frac{2}{N-1}, \quad c_2 = -1 \tag{4.11}$$

For Fig. 4.1(c)

$$\lambda(p,N) = \frac{2(p+1)}{\pi(N-1)^2}, \quad c_1 = \frac{\sqrt{2}}{N-1}, \quad c_2 = \frac{-1}{\sqrt{2}} \tag{4.12}$$

One of the main difficulties concerning the use of Zernike moments as features in image analysis applications is the high computation time to derive them. The long computation time to derive the Zernike moments is due to the factorial terms in the radial polynomials. The computation of factorial terms also leads to numerical instabilities for higher order moments. Hence, it is required to compute the Zernike radial polynomial which require less computation time.

4.1.1 Hybrid Algorithm

The hybrid algorithm used for computing the full set of Zernike moments consists of Prata's simplified Kinther's method and coefficient methods. The hybrid algorithm uses most of Prata's method followed by coefficient and simplified Kintner's methods in computing the Zernike moments.The Prata's recurrence relation is selected as the main component of this hybrid algorithm due to its linear relation between Zernike radial polynomials and less recurrence coefficients as compaired with other recurrence relations.

Whenever Prata's method is not applicable in such cases as $(p = q)$ and $(q = 0)$, the coefficient and simplified Kinther's methods are used. The coefficient method is used for cases where $(p = q)$ and simplified Kinther's method is used to derive the radial polynomials with cases $(q = 0)$ except for $R_{2,0}$ due to its limitations. Zernike radial polynomial for $R_{2,0}$ is solved using coefficient method. The hybrid algorithm for computation of full set of radial polynomials is summarized below.

Step-I: For cases $(p = q)$, Zernike radial polynomial are derived using the equation(3.46.) from the coefficient method

$$R_{pp}(r) = r^p$$

Step-II: For the case of R_{20},Zernike radial polynomial are derived using the equation(3.47) from the coefficient method

$$R_{p(p-2)}(r) = pR_{pp}(r) - (p-1)R_{(p-2)(p-2)}(r)$$

Step-III: For cases $(q = 0)$ except R_{20}, Zernike polynomials are derived using the simplified Kinther's method

$$R_{pq}(r) = (M_1 r^2 + M_2)R_{(p-2)q}(r) + M_3 R_{(p-4)q}(r)$$

Step-IV: For renmaining cases, Zernike polynomials are calculated using the Prata's method

$$R_{pq}(r) = L_1 R_{(p-1)(q-1)}(r) + L_2 R_{(p-2)q}$$

By using the hybrid algorithm, the full set of Zernike moments is obtained through the recurrence relations between its radial polynomials without using any of factorial terms. The hybrid algorithm perform better than other existing fast computation methods due to fewer recurrence coefficients and the linear relation in Prata's method. Fewer recurrence coefficients reduce the number of multiplication in computing tha Zernike radial polynomials while the linear relation reduces the process of computing the power series of radius.

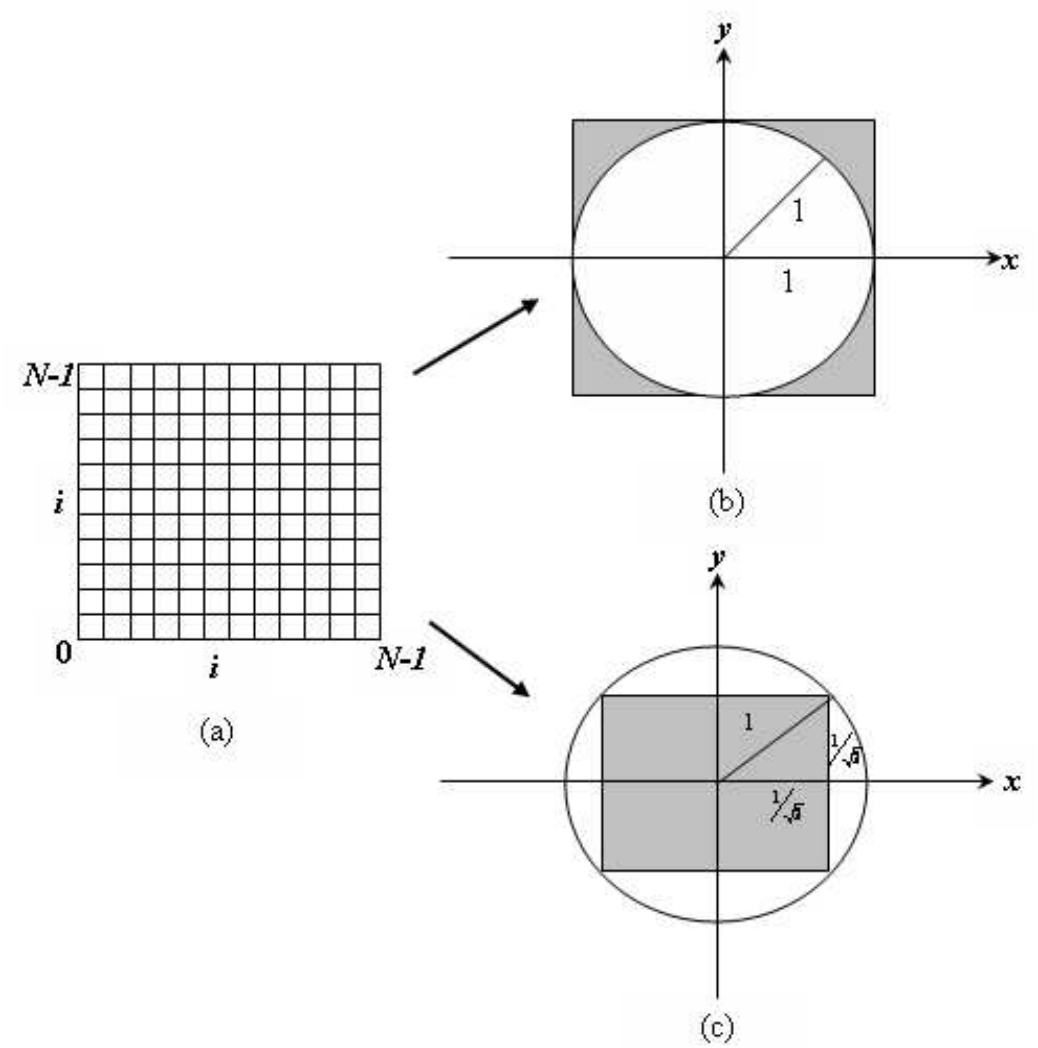

Fig.4.1(a) Image plane NxN, (b) mapping of image plane NxN over a unit circle and (c)mapping of image plane NxN inside a unit circle.

4.2 RECONSTRUCTION USING PSEUDO-ZERNIKE MOMENTS

In similar manner like Zernike moments, images can be reconstructed easily from finite set of Pseudo-Zernike moments. Infact accuracy of reconstruction using Pseudo-Zernike moments is better than that of Zernike moments. Pesudo-Zernike moments have better feature representation capability, and are more robust to image noise than those of convensional Zernike moments.

4.2.1 p-recursive Method

The drawdacks of coefficient method can be avoided by using this p-recursive method. This method uses recurrence relation for Pseudo-Zernike radial polynomials. $R_{pq}(r)$, to accelerate the computation of Pseudo-Zernike moments. The recurrence relation associates $R_{pq}(r)$ with combination of $R_{p-1)q}(r)$ and $R_{(p-2)q}(r)$, which is given as follows:

$$R_{pq}(r) = (M_1 r + M_2) R_{(p-1)q}(r) + M_3 R_{(p-2)q}(r) \tag{4.13}$$

where the coefficient M_1, M_2 and M_3 are given by

$$M_1 = \frac{(2p+1)(2p)}{(p+q+1)(p-q)} \tag{4.14}$$

$$M_2 = -2p + \frac{(p+q)(p-q-1)}{2p-1} M_1 \tag{4.15}$$

$$M_3 = (2p-1)(p-1) - \frac{(p+q-1)(p-q-2)}{2} M_1 + 2(p-1) M_2 \tag{4.16}$$

The initial values for Eq.(4.13) in cases where $p = q$ and $p - q = 1$ can be obtained using the following equations:

$$R_{pp}(r) = r^p \tag{4.17}$$

$$R_{P(p-1)}(r) = (2p+1) R_{pp}(r) - 2p R_{(p-1)(p-1)}(r) \tag{4.18}$$

The complexity of computing Pseudo-Zernike moments of order $\leq p$ using p-recursive method is $O(N^2p^2)$. This method provides a recursive scheme over order p except in cases when $(p-q \leq 1)$. For such a result, R_{00}, R_{11} and R_{10}, etc. are obtained using Eqs.(4.17) and(4.18). These initial values are then used to derive the remaining polynomials with conditions $(p-q > 1)$ using Eq(4.6)

There is no factorial function involved in the p-recursive method. Fast computation is achieved since the calculation of power of radius, r^k, and polynomial coefficients, B_{pqk}, are not required in computing $R_{pq}(r)$. Moments computed using Eq.(4.6) will there fore avoid large variation in the dynamic range of values for different orders of p.This method is useful in applications where fixed polynomial index q is needed.

4.3 RESULTS AND DISCUSSION

In simulation gray image aswell as binary images are considered. Zernike and Pseudo-Zernike moments has been used to reconstruct the images. Hybrid algorithm and p-recursive algorithm as presented in section 4.1 and section 4.2 is used to reconstruct the images Fig.4.1 shows gray scale images reconstructed with different order of moments. As observed fromb Fig.4.1, the aeroplane flying could be reconstructed using 50th order moments while with lower order moments the edges of higher frequency components of the images are missing. This is quite evident from Fig.4.1(f). This phenomenon is different in case of binary aeroplane image as shown in Fig.4.2. The images with hazy edges could be reconstructed with ever 15th order moments. Sharper edges that represent the high frequency component reconstructed with 25th and 50th order moment. The reconstructed image could preserve edges. This is the evident from the Fig.4.2(f) and Fig.4.2(g). Hence, for gray scale im-

ages much higher order moments are neccesary to reconstruct the images. In case of Zernike moments, the image reconstruction needs much higher order as compare to Pseudo-zernike moments. This is depicted in Fig.4.3(b) and Fig.4.3(d). It can be observed from this figure that even with 15th order moments the reconstructed image is loosing edges while 20th Pseudo-zernike moments could yield better results as seen from Fig.4.2(f). Analogus observation is also made for the bottle images. Hence, Pseudo-zernike moments are more appropiate for image reconstruction than Zernike moments.

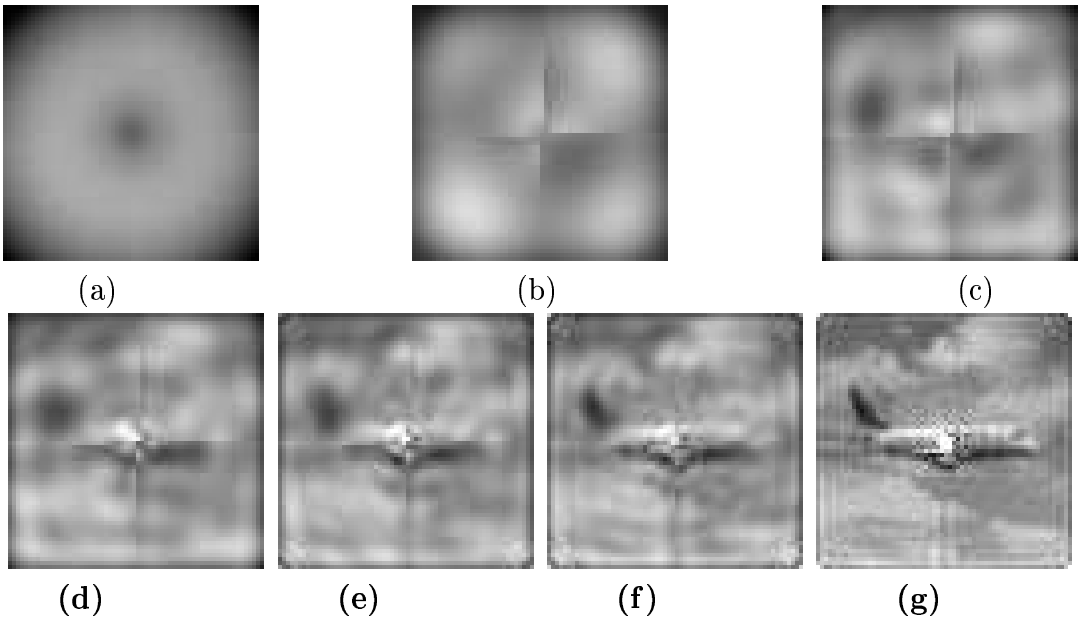

Figure 4.1: Recostruction of the 100x100 image aeroplane in using pseudo-zernike moment of different order,reconstructed images upto order 2nd,5th,10th,15th,20th,25th,50th respectively a,b,c,d,e,f,g

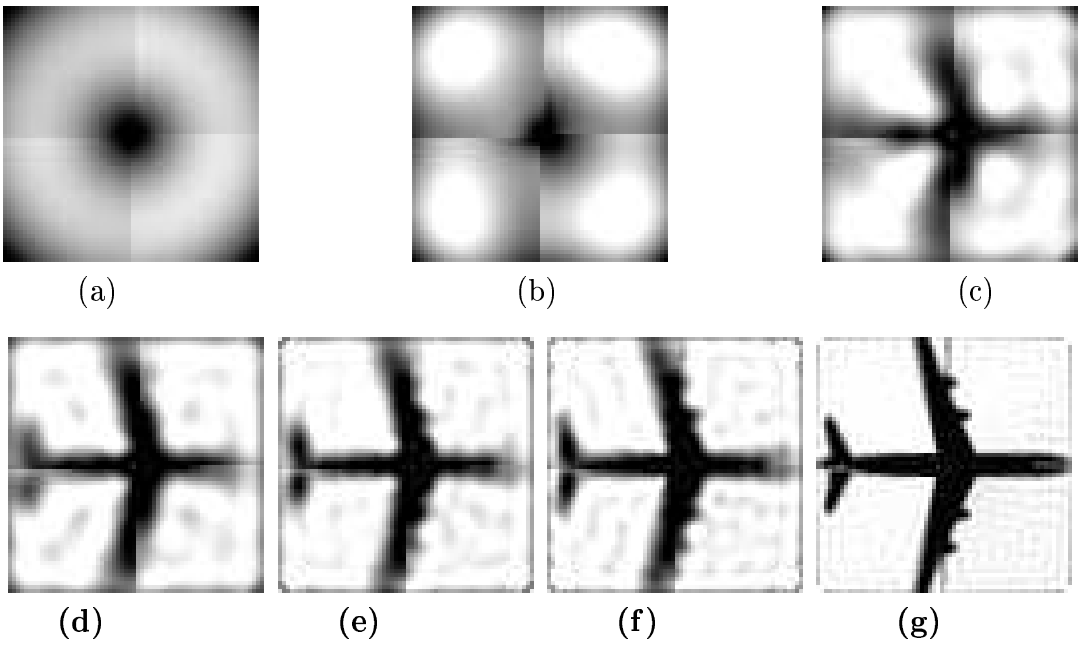

Figure 4.2: Recostruction of the 100x100 image aeroplane in using pseudo-zernike moment of different order,reconstructed images upto order 2nd,5th,10th,15th,20th,25th,50th respectively a,b,c,d,e,f,g

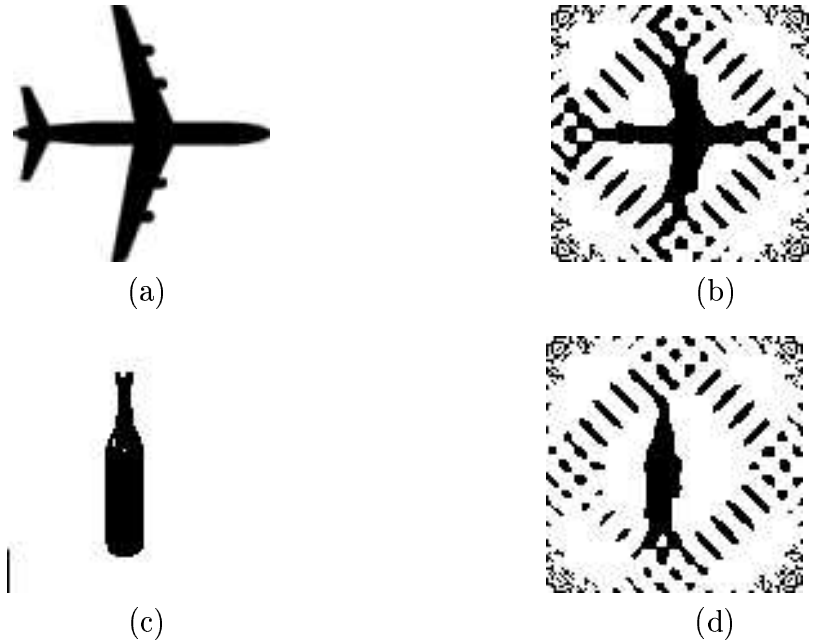

Figure 4.3: Recostruction of the 100x100 images in using Zernike moment of different order,reconstructed images order 50th respectively a,b,c,d

Chapter 5

CONCLUSIONS

In this thesis,the problem of object recognition using moments has been investigated. The The translation,rotation and scalling properties of Geometric moments are studied. The invariance properties of the Geometric moments, specifically central moments are used for recognition. This problem is addressed keeping in view of a machine vision system. Indoor as well as outdoor images are considered for experimentation. Different occlusion are created normally and the correponding Geometric moments are computed. Feedforward multilayered ANN is used for training as well as prediction different occluded version of the images. Although this has been tested for a specified images,this notion can be extended to a class of images. It is observed that ,the trained ANN could yield correct moments for a wide variety of occlusion. This implies that objects occluded from different view pointa can be recognised object,other than trained object could not be recognized. The scheme could be succesfully tested for indoor as well as outdoor objects. The problem of considering a large ANN for prediction of large moments for the proposed of image reconstruction will be pursued. The problem of image reconstrution is also studied. It is observed that the Pseudo-zernike moments could be reconstruct better images than that of Zernike moments.

Bibliography

[1] Hu.M.K, "Visual Pattern recognition By Moment Invariants," IRE Transactions on Information Theory, vol. IT-8, pp. 179-187, Feb. 1962.

[2] Reiss.T.H, "The Revised Fundamental Theorem of Moment Invariants," IEEE Transactions on Pattern Analysis and Machine Intelligence, vol. PAMI-13, no. 8, pp. 830-834, Aug. 1991.

[3] Raveendran.P,Jegannathan.P and Omatu,S, "Classification of Elongated and Contracted Images using New Regular Moments," In IEEE World Congress on Computation, Orlando, FL, June 26-July 2, pp.4154-4158, 1994.

[4] Suk.T and Flusser.J, "Blur and Affine Moment Invariants," 16th International Conference on Pattern Recognition, ICPR-02, vol.4, pp.339-342, 2002.

[5] Tianxu.Z and Jin.L, "Blured Image Recognition based on Moment Invariants," International Conference on Image Processing, ICPR-04, pp.2131-2134, 2004.

[6] Teh.C and Chin.R.T,"On Image Analysis by the methods of moments," IEEE Transactions on Pattern Analysis and Machine Intelligence, vol. PAMI-10, no. 4, pp. 496-513, July 1988.

[7] Khotanzad.A and Hong.Y.H,"Invariant Image Recognition by Zernike Moments,"IEEE Transactions on Pattern Analysis and Machine Intelligence, vol. PAMI-12, no. 5, pp. 489-497, May 1990.

[8] Chong.C,Raveendran.P and Mukundan.R,"A Comparative Analysis of Algorithms for Fast Computation of Zernike Moments,"Pattern Recognition, vol.36, no. 3, pp. 731-742, 2003.

[9] Wee.C, Raveendran.P and Takeda.F, "New computational Methods for Full and Subset Zernike Moments,"Pattern Recognition, vol.159, no. 8, pp. 203-220, 2004.

[10] Chong.C, Mukundan.R and Raveendran.P,"An Efficient Algorithm for Fast Computation of Pseudo-Zernike Moments," International Jornal of Pattern Recognition and Artificial Intelligence, vol. 17, no. 6, pp. 1011-1023, Sept. 2003.

[11] Mukundan.R, Ong.S.H and Lee.P.A,"Image Analysis by Tchebichef Moments,"IEEE Transactions on Image Processing, vol. 10, no. 9, pp. 1357-1364, Sept. 2001.

[12] Yap.P.T,Raveendran.P and Ong.S.H,"Image Analysis by Krawtchouk Moments,"IEEE Transactions on Image Processing, vol. 12, no. 11, pp. 1367-1377, Nov. 2003.

[13] Yap.P.T,Raveendran.P,"Eigenmoments,"Pattern Recognition,vol.40, pp.1234-1244,2007.

[14] Ping.Z,Ren.H,Zou.Jian,Sheng.Y,Bo.W,"Generic orthogonal moments:Jacobi-Fourier moments for invariant image description,"Pattern Recognition,vol.40, pp.1245-1254,2007.

[15] Mukundan.R, "Some Computational Aspects of Discrete Orthogonal Moments,"IEEE Transactions on Image Processing, vol. 13, no. 8, pp. 1055-1059, Aug. 2004.

[16] Mukundan.R,"Radial Tchebichef Invariants for Pattern Recognition,"IEEE Conference on image processing,TENCON-2005.

[17] Haykin,Simon,"Neural Networks,Pearson Education Inc.,2004